ABSTRACT

Title of Document: SIMULATION OF ABSORPTION CYCLES FOR INTEGRATION INTO REFINING PROCESSES

Christopher Somers, Masters of Science, 2009

Directed By: Dr. Reinhard Radermacher, Mechanical Engineering

The oil and gas industry is an immense energy consumer. Absorption chillers can be used to recover liquid natural gas (LNG) plant waste heat to provide cooling, which is especially valuable in the oil and gas industry and would also improve energy efficiency. This thesis details the modeling procedure for single and double effect water/lithium bromide and single effect ammonia/water chillers. Comparison of these models to published modeling results and experimental data shows acceptable agreement, within 5% for the water/lithium bromide models and within 7% for the ammonia/water model. Additionally, each model was integrated with a gas turbine as a waste heat source and parametric studies were conducted for a range of part load conditions, evaporator temperatures, and ambient conditions. Finally, the best chiller design was selected among the three evaluated here, and an annual performance study was conducted to quantify the expected cooling performance and related energy savings.

MODELING ABSORPTION CHILLERS IN ASPEN

By

Christopher Michael Somers

Thesis submitted to the Faculty of the Graduate School of the
University of Maryland, College Park, in partial fulfillment
of the requirements for the degree of
Master of Science
2009

Advisory Committee:
Professor Reinhard Radermacher, Chair/Advisor
Professor Gregory Jackson
Professor Peter Rodgers

Acknowledgements

My thanks go to Dr. Radermacher for giving me the opportunity to be a part of the Center for Environmental Energy Engineering, to my office mates and colleagues for making my time here worthwhile, and to my family for their love and support.

Table of Contents

List of Tables

List of Figures

Nomenclature

Abbreviations:

Abs	Absorber
ABSIM	Absorption Simulation
APCI	Air Products and Chemicals, Incorporated
COP	Coefficient of performance
Cond	Condenser
Des	Desorber
EES	Engineering Equation Solver
Evap	Evaporator
GE	General Electric
H	High pressure
I	Intermediate pressure
ISO	International Organization for Standardization
L	Low pressure
LiBr	Lithium bromide
LMTD	Log mean temperature difference
LNG	Liquid natural gas
MCR	Multi-component refrigerant
MFR	Mass flow rate
NH3	Ammonia
PFD	Process flow diagram
PR-BM	Peng-Robinson-Boston-Mathias
Rect	Rectifier
SHX	Solution heat exchanger
UA	Overall heat transfer coefficient
V/L HX	Vapor/liquid heat exchanger

Parameters/Variables:

E	Energy
P	Pressure

Q	Heat duty
T	Temperature
W	Work
X	Mass fraction
ε	Heat exchanger effectiveness

Subscripts/Stream Names:

1, 2, 3…	State points 1, 2, 3…
TRB	Turbine
WBACK	Back work
WNET	Net work
WSTHEAT	Waste heat

Chapter 1: Introduction

This thesis explores the possibility of using absorption chillers to utilize waste heat in LNG plants. To accomplish this, models were created in ASPEN and a variety of cycle options were considered. The waste heat source investigated was the exhaust stream from a gas turbine, and since gas turbine models are already available, the bulk of the modeling work reported here focuses on developing absorption chiller models.

Waste Heat Utilization

Waste heat, for this study, will be defined as heat in processes that would otherwise be rejected to ambient. The feasibility of waste heat utilization in a process is dictated by the temperature, quantity, and availability of the waste heat source in question. There are a number of benefits to implementing waste heat utilization measures, the primary benefit being a reduction in the energy demand of the process. Increased energy efficiency has a number of ancillary benefits, including reducing primary energy input, reducing carbon dioxide and other emissions, and reducing operating costs. Thus waste heat utilization is an attractive improvement when feasible.

There have been numerous investigations into the feasibility of waste heat for various applications, including water desalination, air conditioning, gas turbine performance improvements, and vapor compression cycle enhancements [1, 2, 3, 4, 5, 6, 7]. However, there have been relatively few studies specifically addressing waste heat utilization in LNG plants.

LNG Plants

77% of LNG plants in operation are based on the APCI design; therefore, the APCI plant design is the focus of this study [8]. A schematic of the APCI liquefaction cycle is shown in the following figure.

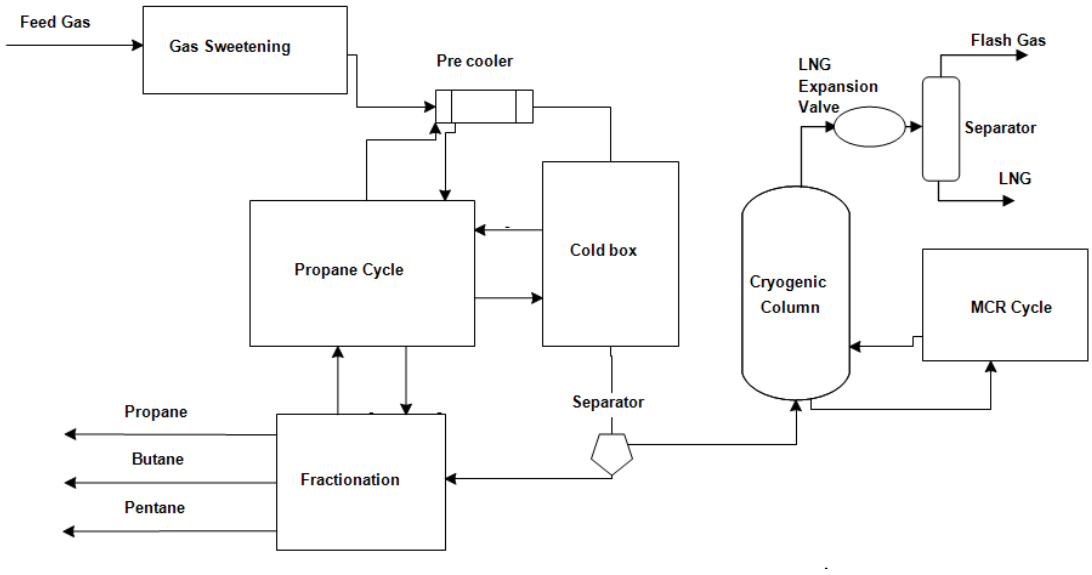

Figure 1: Process flow diagram of an APCI LNG plant [8]

LNG plants are complex because the LNG must be cooled below -160°C. To accomplish this, there are two refrigerant cycles, a propane cycle and a multi-component refrigerant (MCR). The multi-component refrigerant consists of methane, ethane, propane, and nitrogen [9]. The propane and MCR cycles are the focus of this thesis because they meet the plant cooling demand. In total, the cooling load of an APCI cycle is around 180 MW.

Absorption Chillers

An absorption chiller is a closed loop cycle that uses waste heat to provide cooling or refrigeration. Absorption chillers' use has been limited by their relatively poor efficiency at delivering cooling compared to vapor compressions cycles. For comparison, an absorption chiller typically has a coefficient of performance (COP) between 0.5 and 1.5, based on heat input. For comparison, modern vapor compression cycles have COPs in excess of 3.0, based on the input of electric power [10, 11]. However, absorption chillers continue to be viable in some applications because they are able to utilize low temperature (<200°C) heat to provide cooling. In this sense, a COP for an absorption chiller cannot be compared to the COP of other cooling cycles because the input energy for an absorption chiller can be essentially free, for example when it is waste heat, as it would otherwise have been unused in most processes. Thus, in processes where low temperature waste heat is available and cooling is desired, it often makes sense to implement an absorption chiller to increase the overall energy efficiency of the process [12, 13, 14, 15, 16]. Absorption chillers use a refrigerant-absorbent pair as a working fluid. The two most common combinations of working fluids used are water/lithium bromide (LiBr) and ammonia/water. Furthermore, cycles can be half, single, double, or even triple effect. Multi-effect cycles require more components and higher temperature waste heat, but have higher COPs. This thesis focuses on modeling of single effect cycles of both working fluid combinations and double effect water/LiBr absorption chillers.

Modeling History of Absorption Chillers

Absorption chillers have been modeled in the past in a variety of ad hoc programs, such as the one by Lazzarin et al. [17]. Modern modeling is usually done by one of two software: Absorption Simulation (ABSIM), developed by Oak Ridge National Laboratory [18, 19], and Engineering Equation Solver (EES), developed at the University of Wisconsin [20, 21, 22]. EES modeling allows the user to compute thermophysical properties of working fluids, providing results with very good accuracy when compared to experimental results [23].

ASPEN

ASPEN is an engineering software suite. One of these programs is ASPEN Plus, which allows for steady-state process modeling [24]. The user interface is predicated on a library of ready-made, user editable component models based in FORTRAN. By connecting these components by material, heat and work streams and providing appropriate inputs, the user is able to model complex processes. ASPEN is a commonly used software platform for process modeling, particularly in the petroleum industry.

The decision to model absorption chillers in ASPEN, rather than in other available programs, was based primarily on two advantages. First, chiller models produced in ASPEN could be directly integrated with the plant cycle model and with waste heat sources. Secondly, ASPEN has an optimization capability that, when used in future work, will aid in producing the design with the maximum energy savings.

Chapter 2: Motivation and Research Objectives

Motivation

As discussed in the introduction, absorption chillers have been modeled successfully in a number of engineering programs. However, no water/lithium bromide chiller models created in ASPEN Plus have been published in the literature. There is one instance of an ASPEN Plus single effect ammonia/water chiller model in the literature, but this model produced rather large errors (sometimes over 10%) in predicting important parameters such as solution concentrations and component heat duties when compared to experimental data [25]. Thus, accurate ASPEN Plus absorption models would be unique.

Absorption chiller models in ASPEN Plus would have a number of advantages over models in currently used programs like EES. Chiller models created in ASPEN can be integrated directly into other processes modeled in ASPEN. This is important for this project because integrating the chillers directly with the waste heat source and with the plant models give the most accurate and most productive results. Additionally, ASPEN has an optimization capability that will be utilized for considering various configurations, resulting in the maximum benefit from using the available waste heat.

Most importantly, by investigating the option of employing an absorption chiller to use waste heat, one can identify processes whose energy efficiencies are able to be improved. This satisfies the overarching motivation of this project, since

increased energy efficiency means less primary energy input, lower emissions, and cost savings.

Research Objectives

The first research objective was to develop working absorption chiller models in ASPEN Plus. These models were subject to the following constraints:

- There will be a model for each of the following absorption chiller designs: single and double effect water/lithium bromide and single effect ammonia/water.
- The models must be stand-alone, but also capable of being integrated with other models, for example a waste heat source and a gas processing plant.
- The models must only require the following inputs from the user: ambient temperature, waste heat temperature, cooling temperature, heat exchanger effectiveness, and either quantity of waste heat available or desired amount of cooling.
- The models must calculate all outputs of interest, either directly or readily available through simple calculation. Output of interest includes COP, component heat duties, and working fluid state points.
- Models must be verifiable, through comparison with experimental and modeling results from other programs.

The second research objective was to accomplish the following tasks with the working models:

- Each model will be integrated with a waste heat source (i.e. a gas turbine).

- Parametric studies on part load operation, cooling temperature, and ambient temperature will be conducted.
- The various model designs will be subject to a performance comparison, from which the best design based on operating conditions and waste heat available will be selected.
- Finally, the chiller design selected as the best will be subjected to a seasonal study, which will predict how much cooling could be produced throughout operation for a year and related energy savings.

Chapter 3: Water/LiBr Cycle Modeling Approach

Property Method Selection

The first and most crucial step in the modeling process was finding a suitable property method in order to calculate the water/lithium bromide mixture property data. Except for very common fluids, ASPEN does not use look-up tables for property data. Instead, the user must select a property method based on operating conditions and fluid characteristics. As a result, there is an error inherent to any model created in ASPEN, as there is with any property method based modeling software. This is intended as a warning to the potential user to select the property method wisely when modeling in ASPEN, as even look-up tables will have some errors due to interpolation.

To select a suitable property method, the operating conditions and the fluids being modeled were considered. This allowed the number of options to be narrowed to a few methods. From here, simple models were created, and their results compared to expected values. Based on this procedure, the ELECNRTL property method was chosen for the water/lithium bromide solution [26]. It is the most appropriate because it is specifically designed for electrolyte solutions, making it superior to more robust but less specific methods such as Peng-Robinson.

To use ELECNRTL properly, the user must select the relevant components (in this case, water and lithium bromide) and use the electrolyte wizard, which will generate a series of reactions. In this case, the only relevant reaction was the association/dissociation of lithium bromide. For the states that are pure water (7-10),

the steamNBS property method was used in ASPEN [27]. Since look-up tables are available for pure steam, the property data induced error was much smaller than that of the water/LiBr mixture.

In order to verify the accuracy of the ELECNRTL property method in ASPEN, several comparisons were made with the EES property routines. The EES routines are based on a correlation from the 1989 ASHRAE handbook [28]. The range of the both comparisons is restricted by the valid range of the EES correlation Thus, for both comparisons, water/LiBr concentrations between 45% and 75% were considered. The temperature and pressure ranges for both comparisons were selected to correspond with common absorption chiller operating conditions (10°C to 130°C, 0.5 kPa to 100 kPa).

First, both property methods were employed to produce a Dühring Plot [29]. Each was given a variety of temperatures and concentrations of LiBr as inputs and used to find the corresponding saturation pressure. The results of this comparison are shown in Figure 2, with lines of constant concentration from 45% to 70% in 5% increments from left to right. This figure is followed by a graph showing the percent discrepancies between the two property methods.

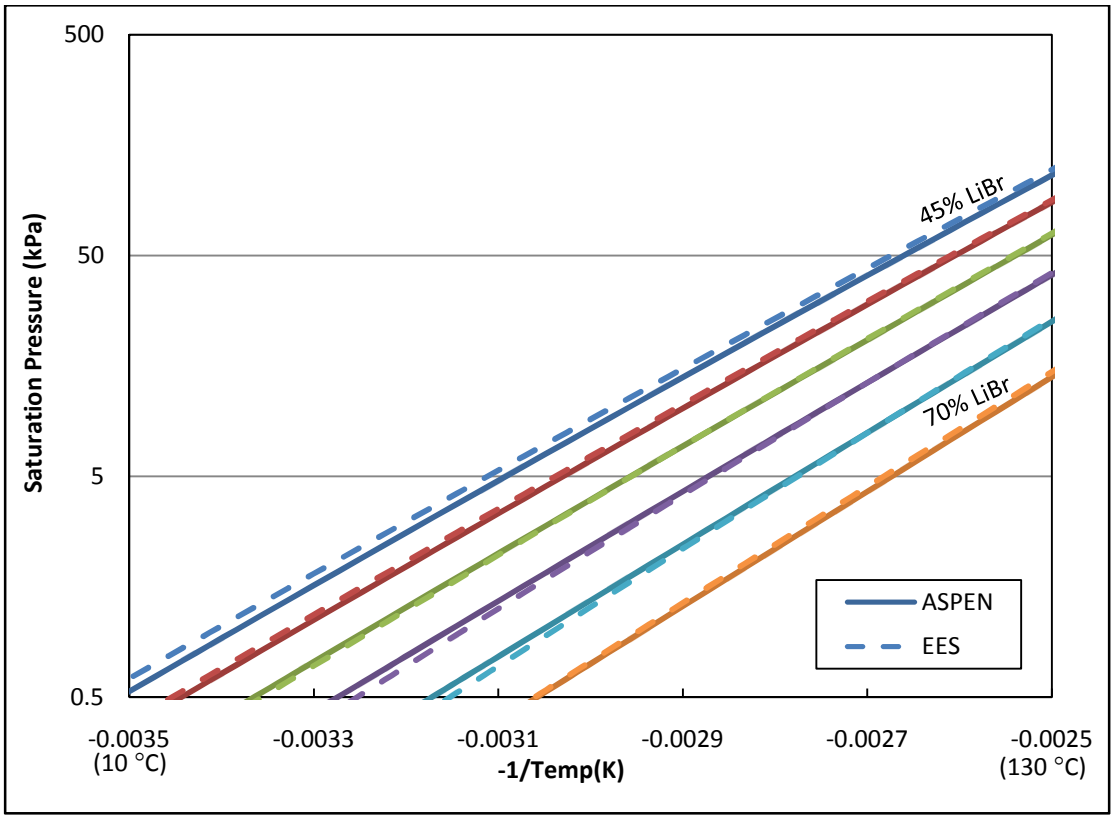

Figure 2: Dühring plot for water/Lithium Bromide using EES and ASPEN

This comparison shows very good agreement between the two property methods. Only the 45% concentration LiBr line shows any significant discrepancy between the EES and ASPEN property methods. Since absorption chillers tend to operate at higher concentrations (in the work detailed in this thesis, 50-65% LiBr), this is not a cause for concern. The average discrepancy in predicted pressure for the entire range of values is 4.4%, but if the 45% concentration line is removed the average discrepancy is only 3.3%. See the following figure for a more specific look at percent discrepancies.

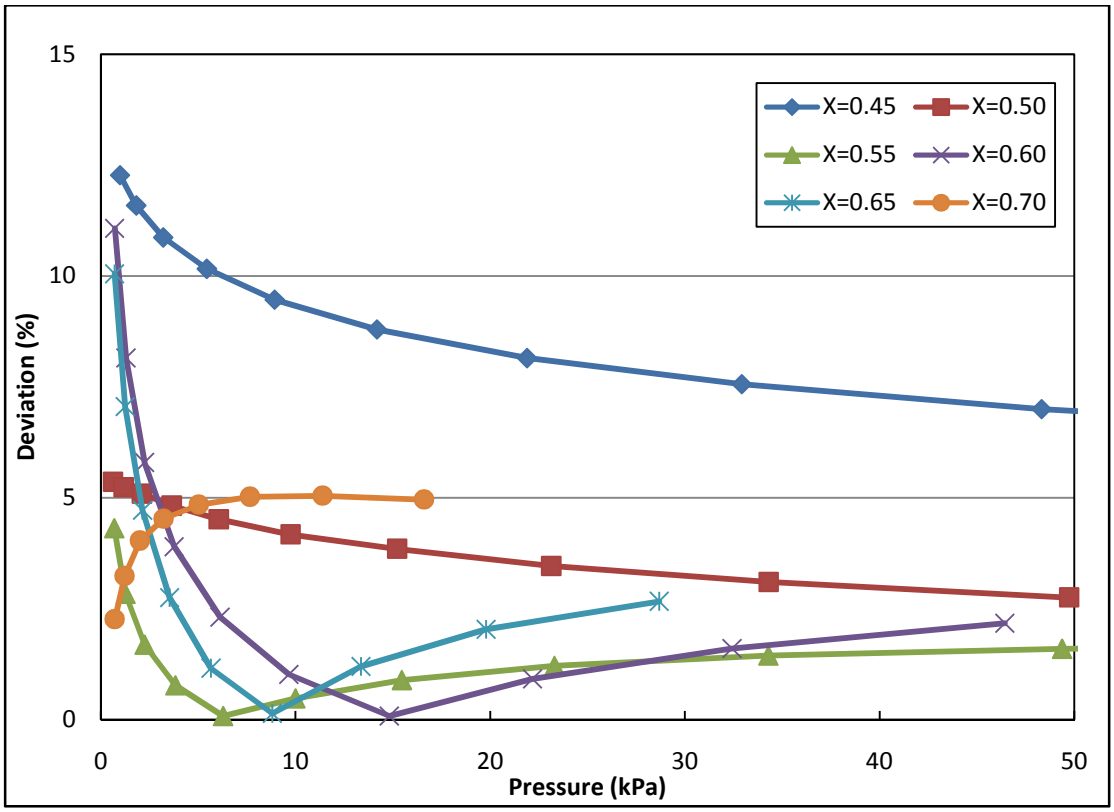

Figure 3: Percent discrepancy in predicting saturation pressure predicted by EES and ASPEN property methods

Figure 3 shows the percent discrepancies between the two property methods in predicting saturation pressure as a function of pressure. It is clear that at higher pressures, the discrepancy is lower. It is also clear that at X=0.45, the discrepancy is by far the worst of any of the concentrations. For all other concentrations, the percent deviation is less than 5% at pressures higher than four kPa.

For the second comparison, both property methods were given a variety of temperatures and pressures as inputs and were used to find saturation concentrations. The EES results were plotted on the x-axis and the ASPEN results on the y-axis. Figure 4 shows that data points are close to the line of zero discrepancy (a line with a slope of one that passes through the origin, upon which two identical property methods' results would fall). The other set of values in the plot show the relative error

of the two methods in predicting saturation concentration. This shows that the two property methods start to have significant discrepancies near 45% LiBr, as evidenced by the data point with nearly 4% error. This is consistent with the findings of the previous comparison, and is likely due to the fact that 45% is the lower boundary of the validity range of the property method used in EES. Other than this single notable point, all other relative errors between the two property methods are below 1.5%.

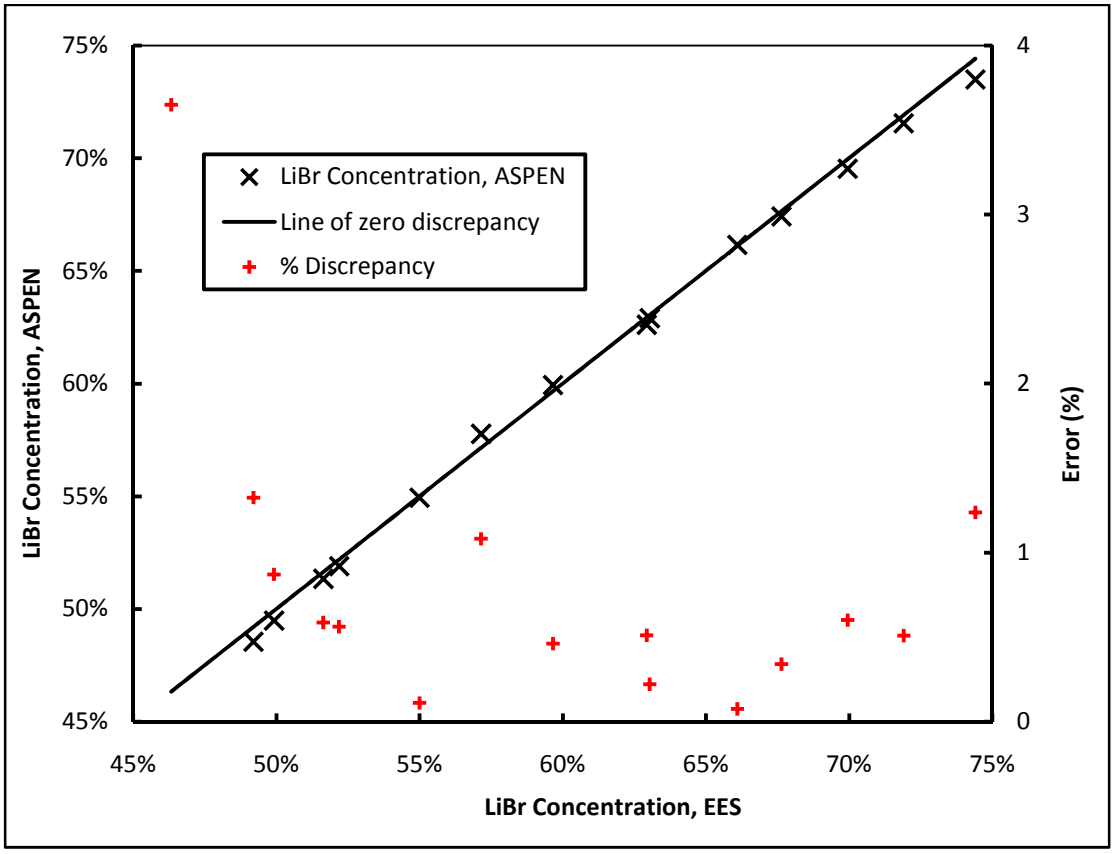

Figure 4: Predicted Water/LiBr concentrations, EES and ASPEN

Based on the favorable comparison with the EES property method, ASPEN's ELECNRTL property method can be used to model water/LiBr mixtures under normal absorption chiller operating conditions.

State Points and Assumptions

The basic operating principle of the absorption cycle is illustrated in Figure 5. Heat is added at the generator (also known as a desorber), separating gaseous refrigerant and liquid solution. The gaseous refrigerant is sent to the condenser, where it rejects heat to a medium temperature sink, usually ambient. It is expanded and then evaporated using heat input from low temperature, which results in useful cooling. The solution is also expanded, and then recombines in the absorber. Normally, a solution heat exchanger (SHX) is also included for increased performance. The hot side of the SHX is placed between the liquid exit of the generator and the solution expansion valve. The cold side is placed between the exit of the pump and the entrance to the generator.

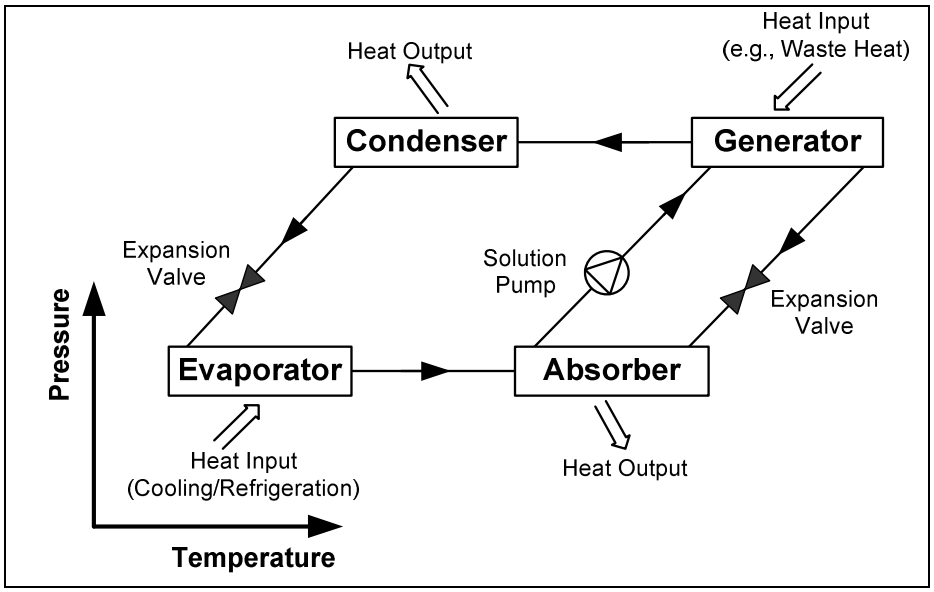

Figure 5: Absorption cycle operating principle [30]

A double effect absorption cycle operates under the same principle, except that a higher pressure level is added. Some of the solution leaving the desorber is pumped to a higher pressure desorber. The resultant refrigerant is condensed in the

higher pressure condenser and fed to the low pressure condenser. The solution exiting the higher pressure desorber is sent back to the low pressure desorber. Finally, in a double effect cycle, the external heat is added to the higher pressure desorber, while the higher pressure condenser rejects heat to the low temperature desorber.

For expediency, the following convention will be used for state points and will be adhered to throughout the paper for the water/LiBr designs. For the single effect cycle, the absorber exit is state 1, the pump exit is state 2, the solution heat exchanger exit leading to the desorber is state 3, the liquid exit of the absorber is state 4, the solution heat exchanger exit leading to the solution valve is state 5, the solution valve exit is state 6, the gas exit of the desorber is state 7, the condenser exit is state 8, the refrigerant valve exit is state 9, and the evaporator exit is state 10. For the double effect cycle, states 1-10 describe the lower pressure half of the cycle and are identical to the states of the single effect cycle. States 11-19 describe the higher pressure side of the cycle using the same numbering system (i.e. state 11 is equivalent to state 1). The following basic assumptions in Table 1 were made for the single effect cycle. A similar set of assumptions were made for the double effect cycle, as enumerated in Table 2. Further assumptions or modeling decisions will be explained in greater detail in following sections.

Table 1: State point assumptions for the single effect water/LiBr cycle

State(s)	Assumption
1	Saturated liquid
2	Determined by the solution pump model
3	Determined by the SHX model
4 and 7	Saturated liquid and saturated vapor respectively; the mass flow rate ratio between states 4 and 7 is determined by the temperature of the waste heat available
5	Determined by the SHX model
6	Determined by the solution valve model
8	Saturated liquid
9	Determined by the refrigerant valve model
10	Saturated vapor

Table 2: State point assumptions for the double effect water/LiBr cycle

State(s)	Assumption
1	Saturated liquid
2	Determined by the lower pressure solution pump model
3	Determined by the SHX model
4 and 7	Saturated liquid and saturated vapor respectively; the mass split between states 4 and 7 is determined by the temperature of the heat coming from the high pressure condenser
5	Determined by the SHX model
6	Determined by the solution valve model
8	Saturated liquid
9	Determined by the refrigerant valve model
10	Saturated vapor
11	Saturated liquid
12	Determined by the high pressure solution pump model
13	Determined by the SHX model
14 and 17	Saturated liquid and saturated vapor respectively; the mass low rate ratio between states 14 and 17 is determined by the temperature of the waste heat available
15	Determined by the SHX model
16	Determined by the solution valve model
18	Saturated liquid
19	Determined by the refrigerant valve model

Both sets of assumptions were chosen because they are commonly used assumptions for absorption chiller modeling [31]. Adhering to the same assumptions as other models commonly make will allow for a conclusive verification of the ASPEN model against other models.

Component Breakdown and Modeling

As alluded to in the introduction, modeling ASPEN plus is based in taking a process and breaking it down into more simple components, also known as "blocks". For example, a gas turbine might be decomposed into a compressor block, a combustion chamber block, and a turbine block. While this allows the user to model complex processes more easily, there is a level of subjectivity involved. Thus, instances when modeling decisions were made will be pointed out and justified when applicable.

The following section is an in-depth description of the component breakdown used to produce the models. It is intended to act as a guide for anyone who wishes to recreate or modify the described models. Many basic components (pumps, valves, etc) might be modeled simply by selecting the equivalent block in ASPEN. The components that did not have exact analogues may have required further assumptions or multiple blocks to model. Finally, it is worth noting that in this section, the goal was only to produce a running model, not one with desired inputs. The adaptation to desired inputs is described later in this chapter.

State Point 1

Because ASPEN uses a sequential solver, it is necessary to model a "break" in closed cycles to give inputs to the model. For both the single and double effect cycles, this break was inserted at state point 1. In other words, the exit of the absorber (stream 1A) and the inlet of the pump (stream 1) are not connected (see the final process flow diagrams at the end of this chapter). If these two fluid streams give the same results (which is to be expected as they represent the same state), this is

evidence of a well formulated problem and that the model converged. This was verified throughout the modeling process and found to be consistently satisfied. The break in state 1 allows for inputs to be given for the pump inlet. For now, these inputs were the low side pressure, a vapor quality of zero, the mass flow rate, and the concentration of water and lithium bromide.

Pumps

Pumps are used between states 1 and 2 in both models and between states 11 and 12 in the double effect model. Pumps require only one input, the exit pressure. One might also include pump efficiency, but the default value of 100% was used because of the negligible effect on the overall cycle of choosing a different efficiency (the pump work is less than 0.1% of the heat duties of the other components). This means that all of the pump work is added directly to the enthalpy of the working fluid, i.e.

$$H_{Out} = H_{In} + W_{pump} \tag{1}$$

Valves

The other pressure change devices needed to model the cycle are valves. For the single effect cycle there is one refrigerant and one solution valve, for the double effect cycle there are two of each. The valve model is self-explanatory; one only needs to give the exit pressure or some equivalent (i.e. pressure ratio). The pump model assumes an adiabatic process, i.e.,

$$H_{In} = H_{Out} \tag{2}$$

Solution Heat Exchangers

A solution heat exchanger (SHX) is used once in the single effect cycle. Heat is transferred from state 4 (the hot side inlet) to state 2 (the cold side inlet), resulting in states 5 (the hot side exit) and 3 (the cold side exit). It is used in the same location in the double effect cycle, as well as to transfer heat from state 14 (the hot side inlet) to state 12 (the cold side inlet) of the higher pressure side, resulting in states 15 (the hot side exit) and 13 (the cold side exit). Each solution heat exchanger was modeled using two heater blocks, connected by a heat stream to indicate that the heat rejected on the hot side was to be added to the cold side. This part of the model is shown in Figure 6. Assuming no pressure drop, the only two unknowns are the exit temperatures. One unknown was described by assuming a heat exchanger effectiveness, defined below.

$$\varepsilon = \frac{T_4 - T_5}{T_4 - T_2} \tag{3}$$

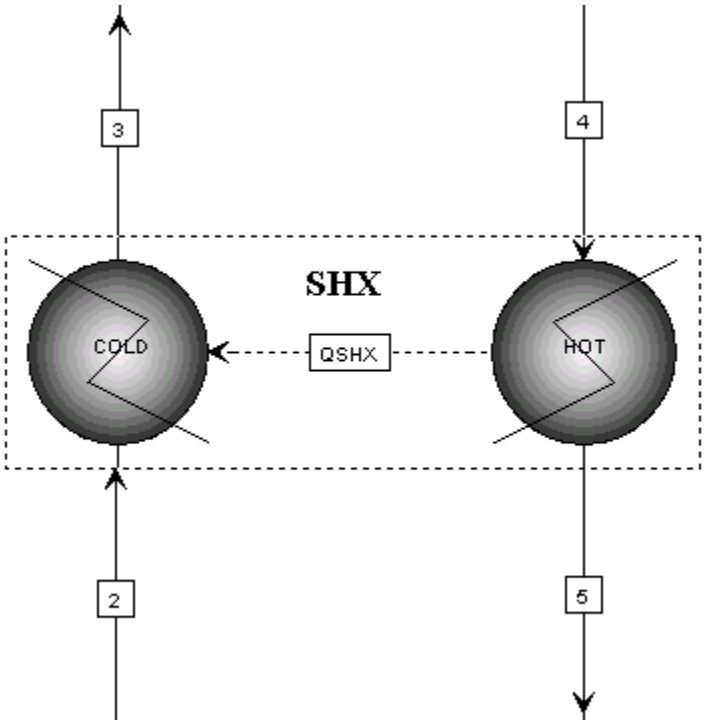

Figure 6: SHX model in ASPEN

This gives T_5, since T_2 and T_4 are known. This equation is implemented in ASPEN using a calculator block. Since three of the four states are now defined, and the heat rejected by the hot side must equal the heat gained by the cold side, T_3 can be calculated by ASPEN. The heat exchanger effectiveness was chosen to be 0.64 to match that of the EES models.

Condensers

The condensers were modeled as heat exchangers. Zero pressure drop was assumed (the merit of this assumption is addressed in chapter 7). The high pressure condenser of the double effect cycle rejects heat to the intermediate pressure desorber. The other condensers reject heat to ambient, in this case seawater. Seawater was modeled as 96.5% water by mass and 3.5% sodium chloride by mass using the ELECNRTL property method. The seawater side of the heat exchanger was assumed

to be raised by 5 K, which allowed the required flow rate to be determined. The refrigerant was assumed to leave the condenser as saturated liquid. Since the refrigerant is pure water the steamNBS property method was used for this component, as well as any refrigerant-only components. The condenser model is used three times, once in the single effect cycle and twice in the double effect cycle (once each at intermediate and high pressures). The intermediate pressure condenser has two refrigerant inlets: the refrigerant coming from high pressure and the refrigerant coming from the intermediate desorber. The condenser model is depicted below.

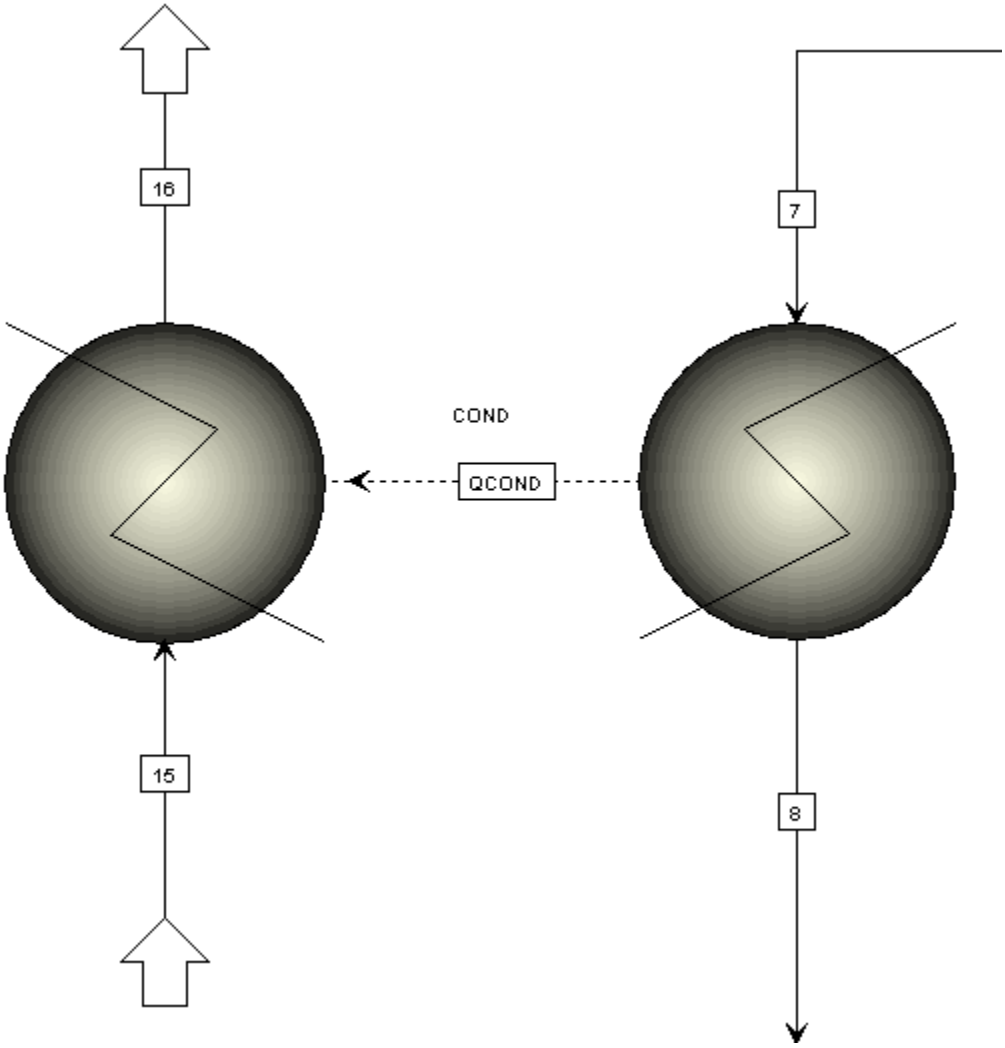

Figure 7: Condenser model in ASPEN

Evaporators

Modeling the evaporators was very similar to modeling the condensers. The evaporator was modeled as a heat exchanger using the steamNBS property method. The inputs to the model were zero pressure drop and a vapor quality of one at the refrigerant exit. In accordance with ASHRAE standards, the cooling medium is pure water that is cooled from 12°C to 7°C. From this restriction, the required flow rate was determined. This model is used one time each in the single and double effect cycles.

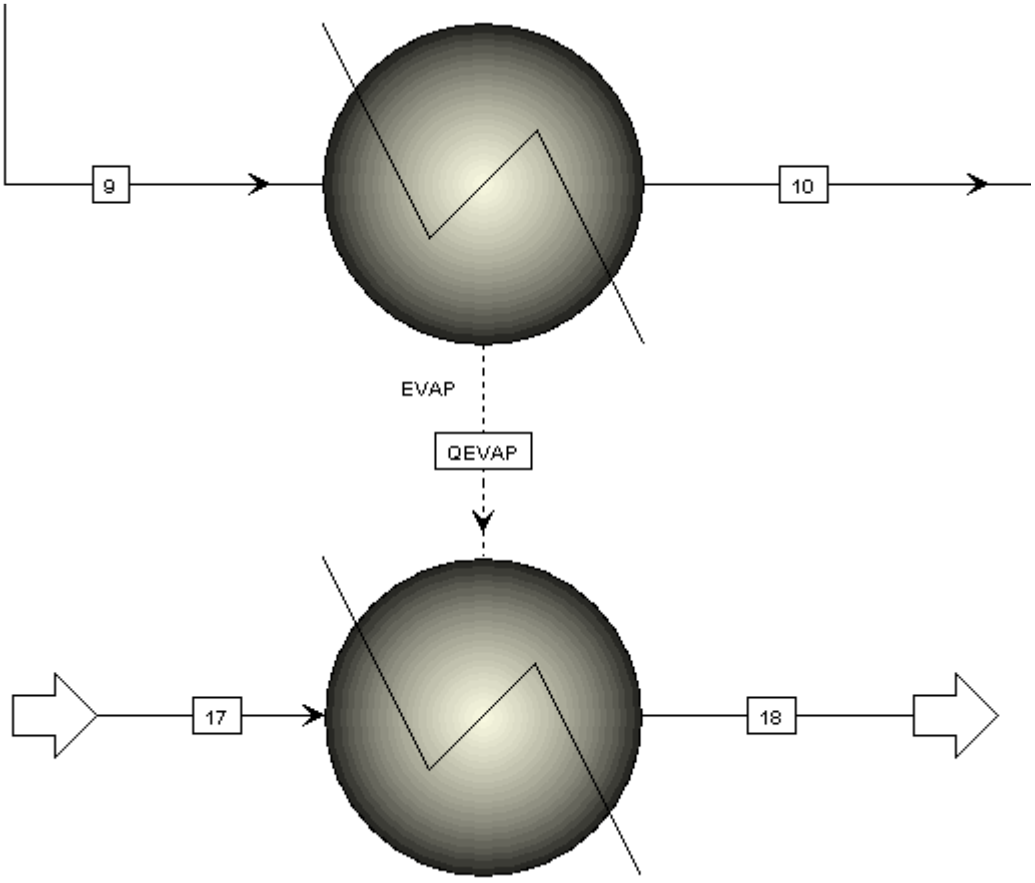

Figure 8: Evaporator model in ASPEN

Absorbers

The absorber is modeled as a heat exchanger with a refrigerant inlet (the exit of the evaporator) and a solution inlet (the exit of the solution valve). Zero pressure drop is assumed, and the solution is assumed to exit as a saturated liquid. Heat is rejected to seawater with a temperature increase of 5 K, which allowed the required flow rate to be determined. The absorber model is used once in the single and double effect cycles.

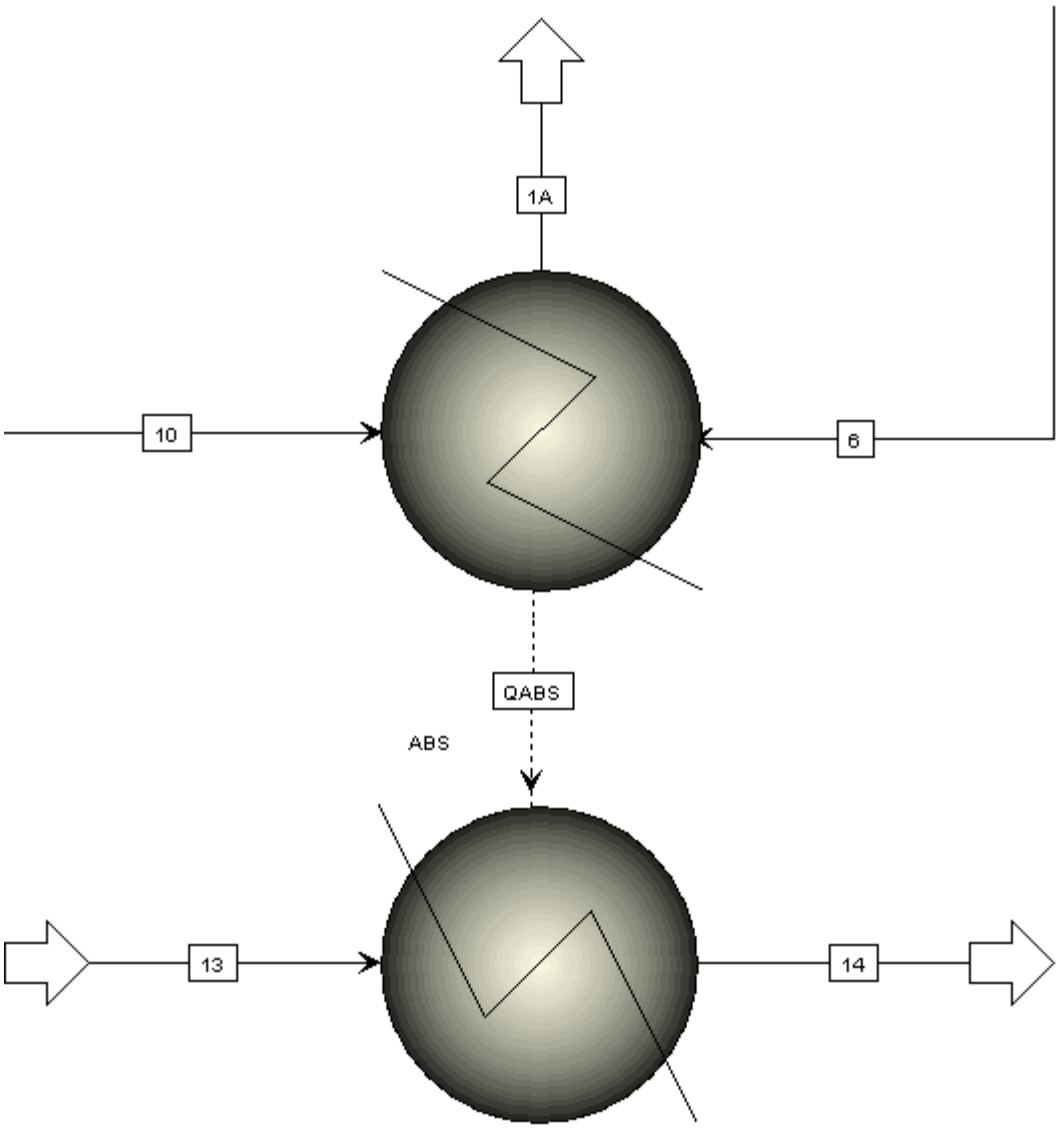

Figure 9: Absorber model in ASPEN

Desorbers

To this point, the modeling of components has been relatively straightforward, as they all involved simple processes such as pressure changes, heat addition or rejection, mixing, or some combination. Desorbers, on the other hand, involve separating components, which makes them much more difficult to model. The desorber in the single effect cycle and the high pressure desorber in the double effect cycle have similar inputs and requirements; thus, they have the same design. They are:

- Single inlet (stream 3 in the single effect, 13 in double effect)
- Saturated vapor outlet (stream 7 in the single effect, 17 in double effect), which is pure water
- Saturated liquid outlet (stream 4 in the single effect, 14 in double effect), which is solution
- Heat source is the gas turbine exhaust

An assumption needs to be made about the vapor outlet stream to define its state. In this model, its temperature was assumed to be the saturation temperature of the liquid solution at state 3 (or state 13, in the double effect model). This was chosen to correspond to the assumption made in the EES model, but could be easily altered [31]. The mass split between the two outlet streams and the liquid output temperature is dictated by the temperature of the heat input to the cycle, which is a given.

To model the solution side of the desorber, three heater blocks and a flash block were used. The flash is used to separate vapor and liquid. Its inputs are zero pressure drop and outlet temperature (based on the temperature of the heat input into

the cycle). However, this gives the vapor stream the same temperature as the liquid stream, which does not meet the assumption stated in the previous paragraph. Thus, a heater block is added to reduce the temperature of the vapor stream to the saturation temperature of the inlet stream. This heat is added at the inlet of the desorber to keep it internal to the desorber, which requires a second heater block at the inlet. The final heater block raises the inlet stream to liquid saturated temperature, which allows a calculator block to reference the liquid saturation temperature of the inlet stream for the purpose of setting the outlet vapor stream temperature.

To model the heat addition, a fourth and final heater block was used, with gas turbine exhaust as its inlet. The exhaust is cooled to a decided upon "useful heat temperature". The model in ASPEN is shown in Figure 10.

The intermediate pressure desorber in the double effect cycle has different inputs and requirements:

- Two inlets (streams 3 and 16)
- Saturated vapor outlet (pure water, stream 7)
- Two saturated liquid solution outlets (stream 11 goes to the higher pressure half of the cycle, and stream 4 goes to the lower pressure half)

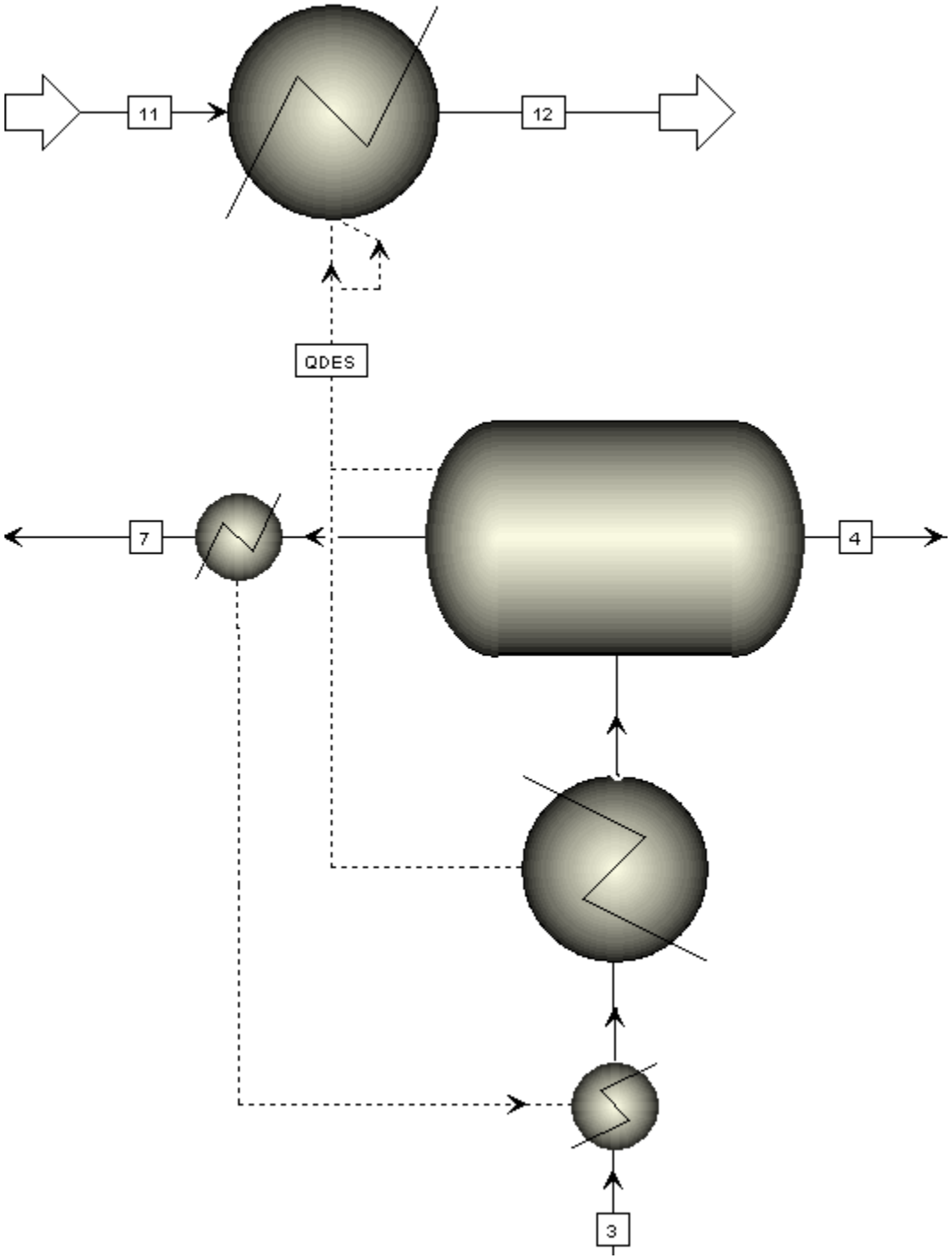

Figure 10: Desorber model for single effect water/LiBr model and for double effect water/LiBr model at high pressure in ASPEN

The intermediate pressure desorber for the double effect model can be seen in

Figure 11. Stream 3 is split based on the requirement that the high pressure condenser

and intermediate pressure desorber have the same magnitude heat duty, accomplished with a splitter block. The solution is raised to saturation temperature with a heater block and is sent to the higher pressure half of the cycle as stream 11. The remaining solution mixes with the other inlet stream. The temperature at which this solution is flashed is based on the assumption that the solution concentrations are the same for both halves of the cycle. Finally, as in the other desorber design, the vapor outlet temperature must be adjusted. Thus, the final heater block sets the outlet temperature equal to the temperature of stream 11 (which is a saturated liquid). The vapor goes to the intermediate pressure condenser and the liquid goes to the lower pressure half of the cycle. For each component, zero pressure drop was assumed.

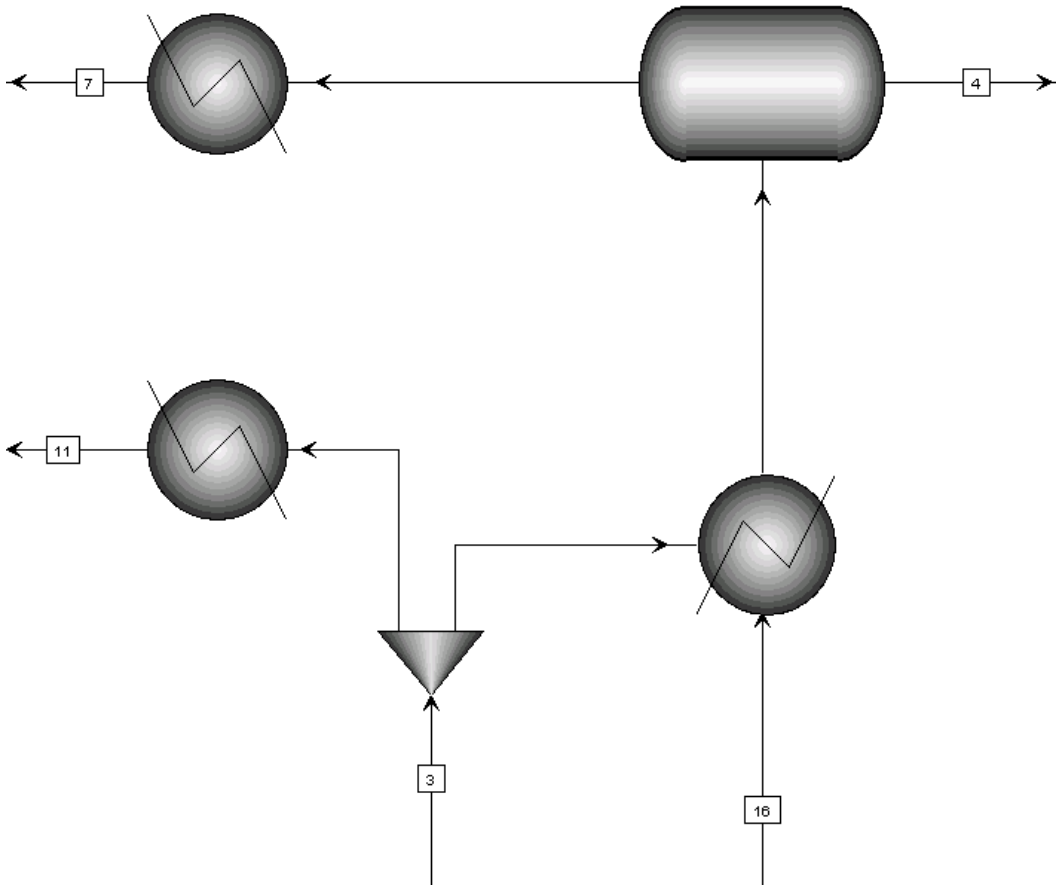

Figure 11: Desorber model for double effect water/LiBr at intermediate pressure in ASPEN

For both of these desorber models, the combination of components is intended to represent the physical desorber. To obtain the heat duty of each desorber, one must add the duties of the individual components of the corresponding desorber model, i.e.

$$Q_{Desorber} = \sum Q_{Desorber\ Components} \quad (4)$$

Adaptation to Desired Inputs

Once the two working models were created, they were adapted to require desired inputs only. Those inputs are:

- Either quantity of waste heat available or desired cooling load
- Evaporator exit temperature (related to desired cooling temperature)
- Condenser and absorber exit temperatures (related to ambient temperature, or whatever other medium they are rejecting heat to)
- (High pressure) desorber exit temperature (related to temperature of available waste heat)

Each of these inputs defines a pressure, concentration, or mass flow rate, as enumerated below. For both cycles, either waste heat available or cooling load defines the mass flow rate through the (lower pressure) pump. For the double effect cycle, the mass split between the higher and lower pressure halves of the cycle is given by the specification that the high pressure condenser and intermediate pressure desorber have the same heat duty. For both cycles, evaporator exit temperature defines the low pressure. For both cycles, absorber exit temperature defines the solution concentration at the absorber exit. In the single effect cycle, the condenser exit temperature defines the high pressure. In the double effect cycle, the intermediate pressure condenser exit temperature defines the intermediate pressure. Both of these

are related to ambient temperature. Also in the double effect cycle, the high pressure condenser exit temperature defines the high pressure. This temperature is based on the temperature of the intermediate pressure desorber (where it rejects heat to), for example by assuming a pinch temperature or an overall heat transfer coefficient (i.e. a UA value). In the single effect cycle, the temperature at the liquid exit of the desorber (related to the temperature of the available heat) defines the concentration at the desorber exit. This can be specified by changing the temperature in the flash block (i.e. a design spec is not necessary). The same is true of the high pressure desorber in the double effect cycle. Finally, the temperature of the intermediate pressure desorber in the double effect cycle is set by assuming the concentration at the liquid exit of both desorbers is the same.

To accomplish the adaptation to desired inputs in ASPEN, the user must define a design spec, instructing ASPEN to vary the appropriate variable so that desired input variable reaches the desired value. For example, to meet the desired cooling load, instruct ASPEN to vary the total mass flow rate until the desired evaporator duty is met.

Complete Models

The complete models in ASPEN are shown in Figure 12 and Figure 13 below. For the double effect cycle, the desorbers were placed in hierarchy blocks to reduce clutter.

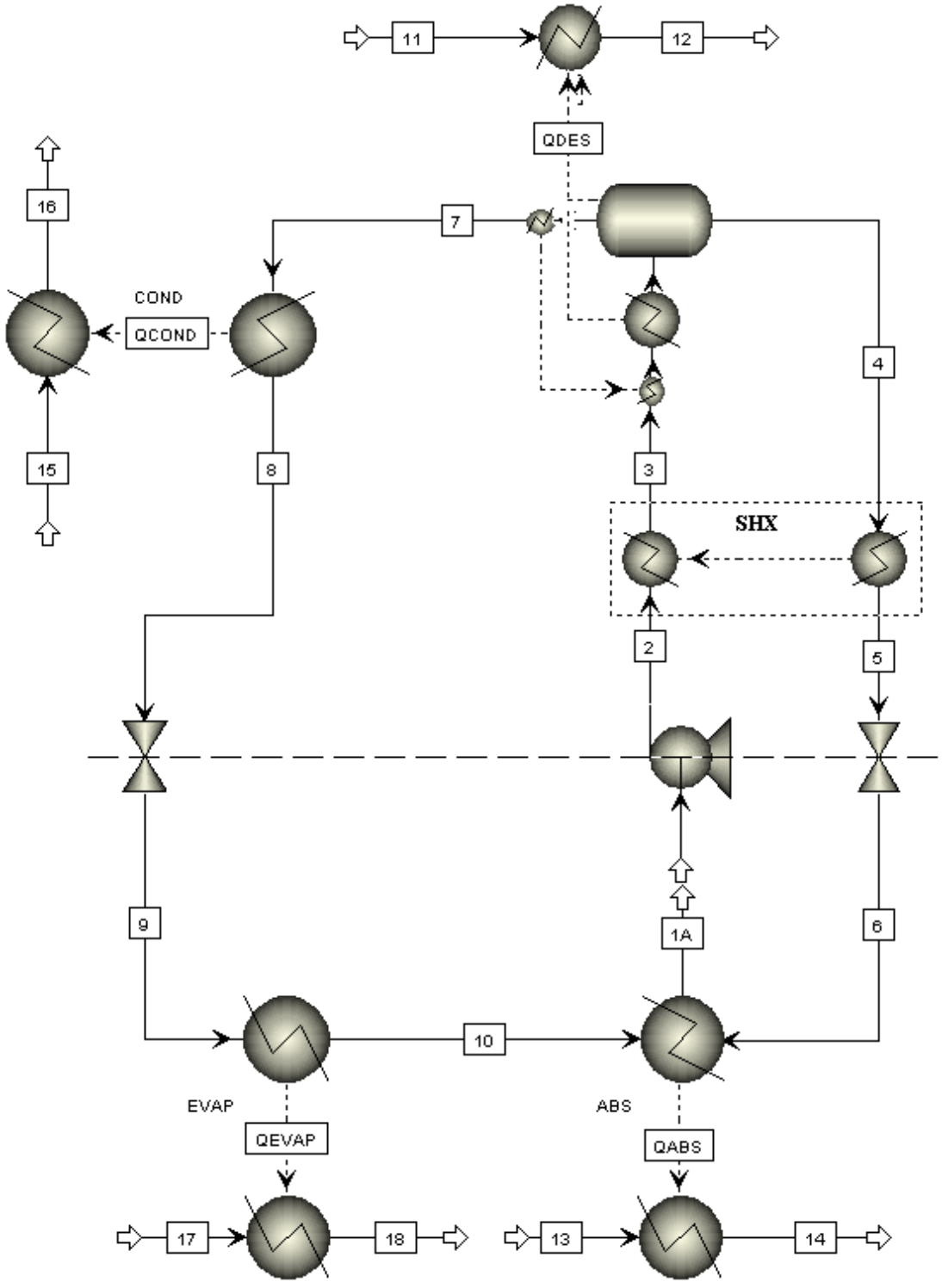

Figure 12: Single effect water/LiBr cycle model in ASPEN

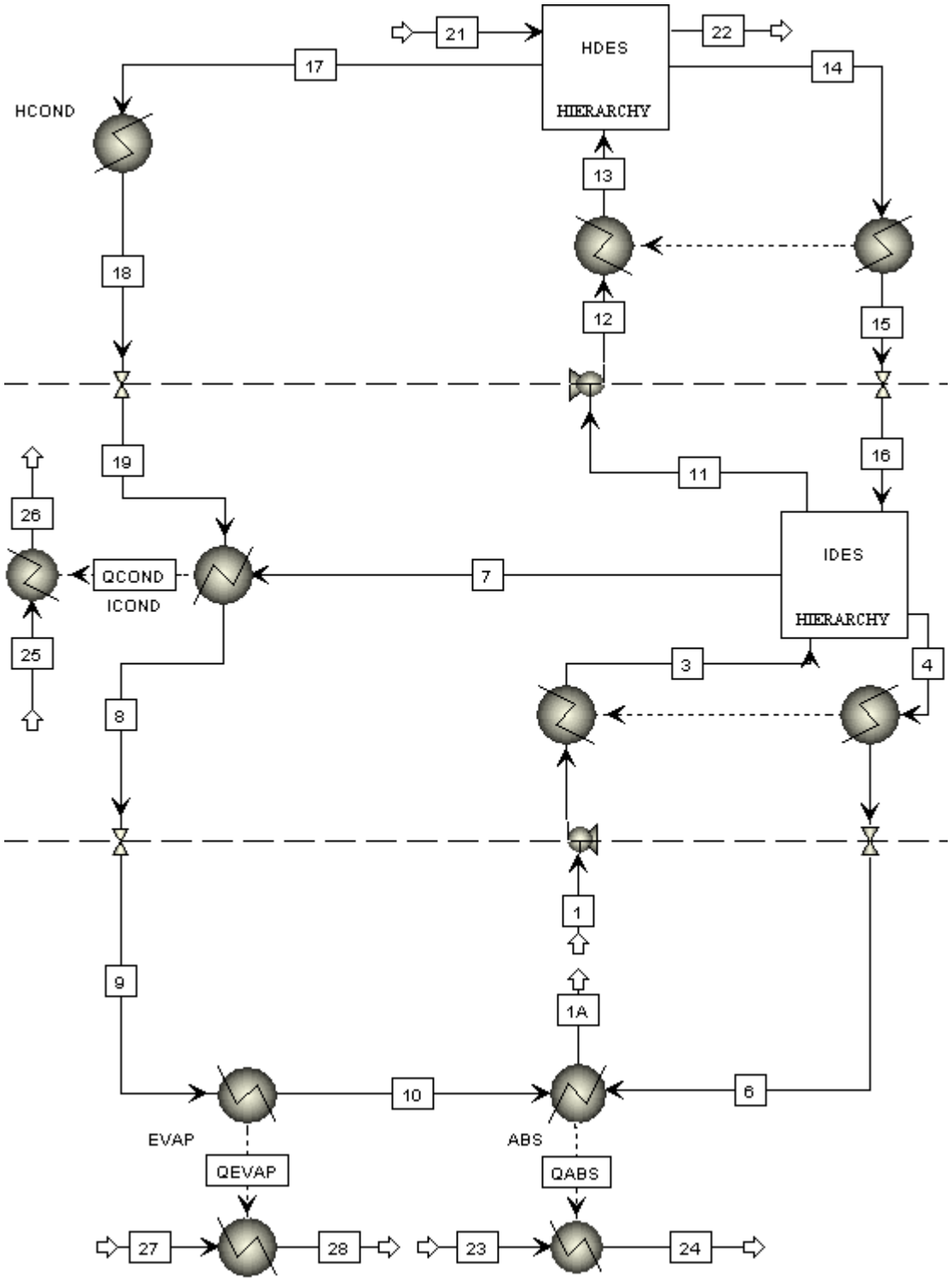

Figure 13: Double effect water/LiBr cycle model in ASPEN

Chapter 4: Ammonia/Water Cycle Modeling Approach

Property Method Selection

As in the water/LiBr model, selecting the correct property method is crucial for getting meaningful results. Unfortunately, while the ELECNRTL method worked well for water/LiBr, it did not make sense to use for ammonia/water so a different method had to be selected. Because a property method specific to these working fluids was not available, a more general method had to be used. Thus, as in the previous paper written on modeling ammonia/water chillers in ASPEN Plus, it was found that Peng-Robinson was the best available method [25, 32].

State Points and Assumptions

The operating principle of the ammonia/water cycle is similar to that of the water/LiBr cycle as discussed in chapter 3. This section will only discuss the differences between the two cycle designs.

There are two major differences between the water/LiBr and the ammonia/water cycles. Firstly, because of the difference in vapor pressures between the two working fluids, it is more difficult to separate ammonia/water in the desorber than in the water/LiBr cycle. Thus, the vapor exit of the desorber is only 90-95% refrigerant, compared to virtually 100% steam for the water/LiBr cycle. This is problematic because a two component refrigerant will have a large temperature glide in the evaporator if evaporated completely (i.e., taken entirely from a quality of zero to a quality of one). Since a temperature glide greater than a few degrees Kelvin is

unacceptable, the working fluid can't be fully evaporated. As a result, the cooling capacity will suffer.

To remedy this issue, a rectifier is used. It is placed after the vapor exit of the desorber to condense some of the non-refrigerant, allowing a much higher percentage refrigerant to go to the condenser. Since the working fluid is a higher percentage refrigerant, the temperature glide will be much less. Thus, the working fluid can be brought to a vapor quality near one and the cooling capacity will be significantly increased. The relationship between percent ammonia and temperature glide is shown in Figure 14 below.

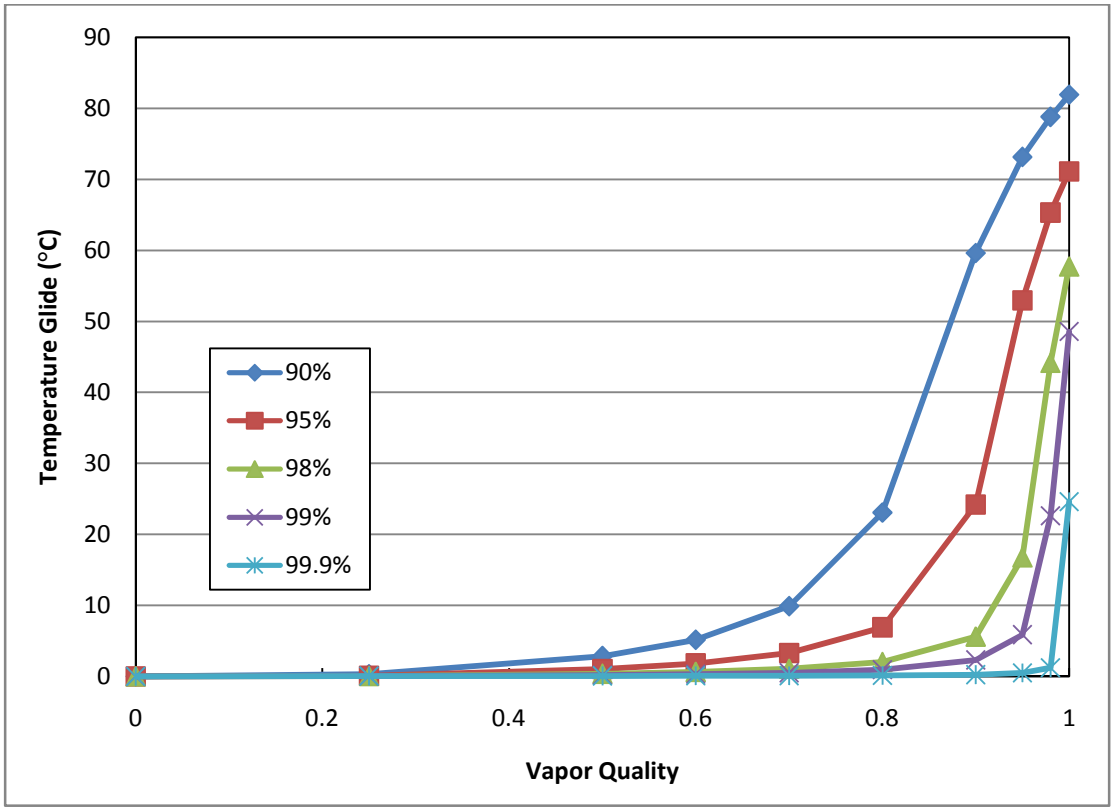

Figure 14: Effect of ammonia concentration on temperature glide of ammonia/water mixture (ASPEN predicted)

The other major difference between the cycles is the addition of a vapor/liquid heat exchanger, which is included for performance enhancement. By placing a heat

exchanger with one side between the condenser and refrigerant valve and the other side after the evaporator, the cooling capacity can be increased appreciably. The vapor/liquid heat exchanger is frequently used in the ammonia/water cycle (and not in the water/LiBr cycle) because ammonia/water has a lower COP and thus there is a greater emphasis performance enhancement. Additionally, the water/LiBr cycle cannot afford the associated pressure drop and would face crystallization issues.

For expediency, the following convention will be used for state points and will be adhered to throughout the paper for the ammonia/water design. The absorber exit is state 1, the pump exit is state 2, the solution heat exchanger exit leading to the desorber is state 3, the liquid exit of the absorber is state 5, the solution heat exchanger exit leading to the solution valve is state 5, the solution valve exit is state 6, the gas exit of the desorber leading to the rectifier is state 7, the exit of the rectifier leading back to the desorber is state 8, the exit of the rectifier leading to the condenser is state 9, the condenser exit is state 10, the vapor/liquid heat exchanger exit leading to the refrigerant valve is state 11 (when applicable), the refrigerant valve exit is state 12, the evaporator exit is state 13, and the vapor/liquid heat exchanger exit leading to the absorber is state 14 (when applicable). The following basic assumptions in Table 3 were made for the single effect cycle. Further assumptions or modeling decisions will be explained in greater detail in following sections.

Table 3: State point assumptions for the single effect ammonia/water cycle

State(s)	Assumption
1	Saturated liquid
2	Determined by the solution pump model
3	Determined by the SHX model
4 and 7	Saturated liquid and saturated vapor respectively; the mass flow rate ratio between states 4 and 7 is determined by the temperature of the waste heat available
5	Determined by the SHX model
6	Determined by the solution valve model
8 and 9	Determined by the rectifier model based on a desired mass percent ammonia in state 9
10	Saturated liquid
11*	Determined by vapor/liquid heat exchanger model
12	Determined by refrigerant valve model
13	Vapor quality determined by evaporator pinch temperature
14*	Determined by vapor/liquid heat exchanger model

This set of assumptions was chosen because they are commonly used assumptions for absorption chiller modeling [31]. Adhering to the same assumptions as other models commonly do will provide verification of the ASPEN model against other models.

Component Breakdown and Modeling

The following section is an in-depth description of the component breakdown used to produce the ammonia/water model. Many basic components (pumps, valves, etc) could be modeled simply by selecting the equivalent block in ASPEN. The components that did not have exact analogues may have required further assumptions

*These state points only exist when the vapor/liquid heat exchanger is included in the cycle

or multiple blocks to model. Finally, it is worth noting that in this section, the goal was only to produce a running model, not one with realistic inputs. The adaptation to realistic inputs is described later in the chapter.

State Point 1

Because ASPEN uses a sequential solver, it is necessary to model a "break" in closed cycles to give inputs to the model. This break was inserted at state point 1. In other words, the exit of the absorber (stream 1A) and the inlet of the pump (stream 1) are not connected (see the overall process flow diagram at the end of the chapter). If these two fluid streams give the same results (which is to be expected; they represent the same state!), this is evidence of a well formulated problem. This was verified throughout the modeling process and found to be consistently satisfied. The break in state 1 also allows for inputs to be given for the pump inlet. For now, these inputs were the low side pressure, a vapor quality of zero, the mass flow rate, and the concentration of water and lithium bromide.

Pump

A pump was used between state 1 and 2. The pump model required only one input, the exit pressure. One could also include pump efficiency, but the default value of 100% was used because of the negligible effect on the overall cycle of picking a different efficiency (the pump work is only a few percent of the heat duties of components like the evaporator and desorber). This means that all of the pump work is added directly to the enthalpy of the working fluid, i.e.

$$H_{Out} = H_{In} + W_{pump}$$

Valves

The other pressure change devices needed to model the cycle are valves. A valve was placed between state points 5 and 6 and between either state points 11 and 12 or 10 and 12, depending on whether a vapor/liquid heat exchanger was included. The valve model is self-explanatory; one only needs to give the exit pressure or some equivalent (i.e. pressure ratio). The pump model assumes an adiabatic process, i.e.,

$$H_{In} = H_{Out}$$

Solution Heat Exchanger

A solution heat exchanger (SHX) is used once. Heat is transferred from state 4 (the hot side inlet) to state 2 (the cold side inlet), resulting in states 5 (the hot side exit) and 3 (the cold side exit). The solution heat exchanger was modeled using two heater blocks connected by a heat stream to indicate that the heat rejected on the hot side was to be added to the cold side. A screen shot of this part of the model is shown in Figure 6 in the previous chapter. Assuming no pressure drop, the only two unknowns are the exit temperatures. One unknown was described by assuming a heat exchanger effectiveness, defined below.

$$\varepsilon = \frac{T_4 - T_5}{T_4 - T_2}$$

This gives T_5, since T_2 and T_4 are known. This equation is implemented in ASPEN using a calculator block. Since three of the four states are now defined, and the heat rejected by the hot side must equal the heat gained by the cold side, T_3 can be calculated by ASPEN.

Condenser

The condenser was modeled as a heat exchanger. Zero pressure drop was assumed. The condenser rejects heat to ambient, in this case seawater. Seawater was modeled as 96.5% water by mass and 3.5% sodium chloride by mass using the ELECNRTL property method. The seawater side of the heat exchanger was assumed to be raised by 5 K, which allowed the required flow rate to be determined. The refrigerant was assumed to leave the condenser as saturated liquid. The condenser model was placed between states 9 and 10. Since the ammonia/water condenser model is identical in appearance to the water/LiBr condenser model, please see the condenser model in the water/LiBr section.

Evaporator

Modeling the evaporator was very similar to modeling the condenser. The evaporator was modeled as a heat exchanger with zero pressure drop. Unlike in the water/LiBr chiller, the vapor quality of the refrigerant cannot be one at the exit because of the temperature glide that will occur due to the presence of water. An acceptable change in temperature across the evaporator was assumed, and this was used to calculate the vapor quality at the exit. In accordance with ASHRAE standards, the cooling medium is pure water that is cooled from 12°C to 7°C. This allowed the required flow rate to be determined. This model was placed between state points 12 and 13. Since the ammonia/water evaporator model is identical in appearance to the water/LiBr evaporator model, please see the evaporator model in the water/LiBr section.

Absorber

The absorber is modeled as a heat exchanger with a refrigerant inlet (the exit of the evaporator) and a solution inlet (the exit of the solution valve). Zero pressure drop is assumed, and the solution is assumed to exit as a saturated liquid. Heat is rejected to seawater with a temperature increase of 5 K, which allowed the required flow rate to be determined. Since the ammonia/water absorber model is identical in appearance to the water/LiBr absorber model, please see the absorber model in the water/LiBr section.

Desorber

The desorber model was not recycled from the water/LiBr model because the binary relationship between the working fluids is different. Thus, a distillation column was used to model the desorber, which is shown in Figure 15 below. Again, zero pressure drop is assumed. For the solution side, bottoms rate is used as an intermediate input; later, a design spec will be used to make temperature an input. On the heat addition side, the gas turbine exhaust is cooled to a decided-upon "useful heat temperature" and the heat rejected from the exhaust heats the desorber.

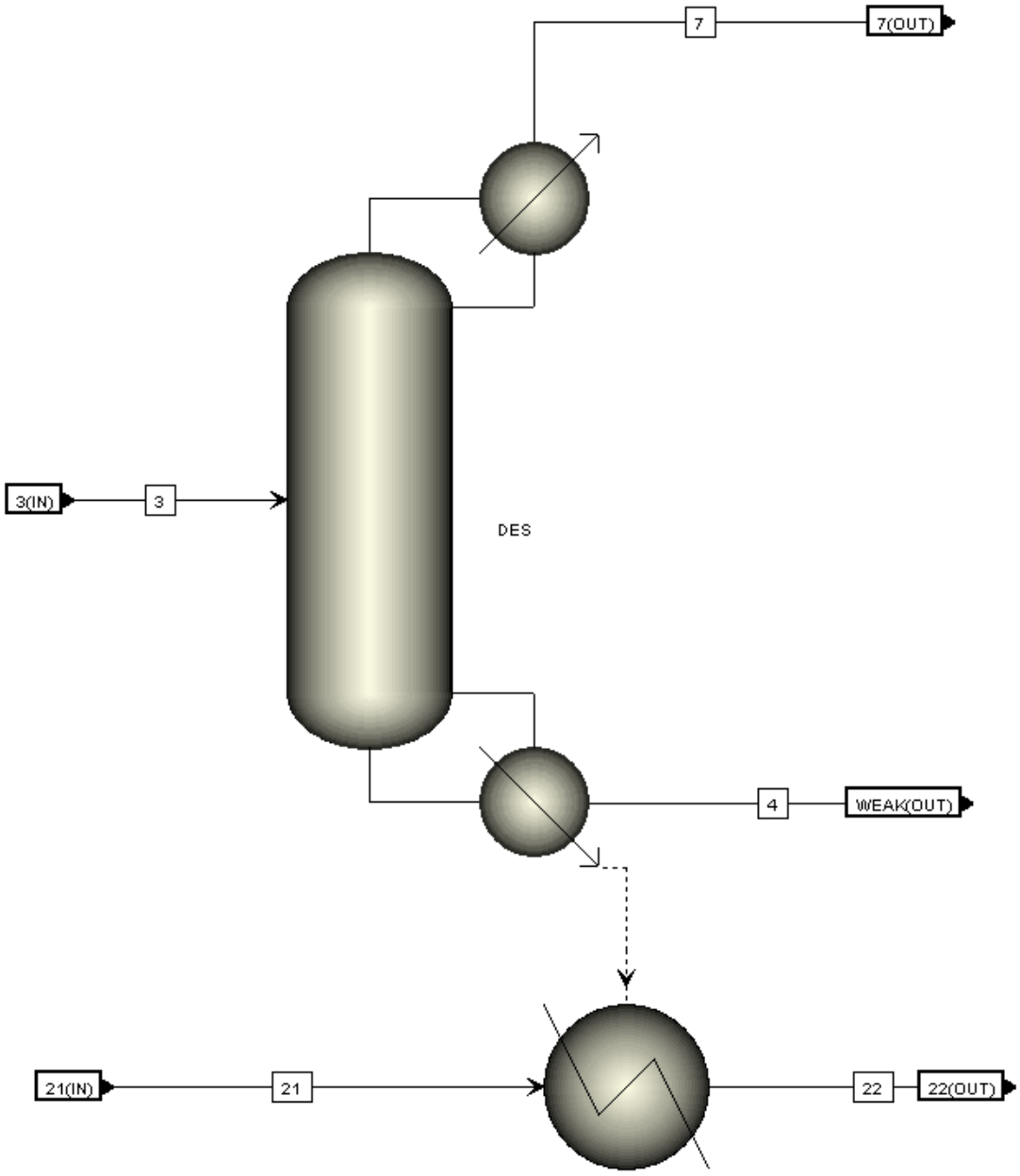

Figure 15: Ammonia/water desorber model in ASPEN

Rectifier

The rectifier is placed at the vapor exit of the desorber. Its function is to condense out some of the solution, leaving higher percentage ammonia, the benefits of which are discussed earlier in the chapter. This is accomplished using a flash block, with inputs of zero pressure drop and heat duty. Heat duty is an intermediate

input; as discussed later in the chapter, a design spec is created to make mass percentage ammonia an input. The liquid exit of the rectifier (state point 8) combines with the liquid exit of the desorber to form state 4 and the gaseous exit of the rectifier goes to the condenser as state point 9. At this point, it is worth pointing out that the definitions of state point 8 and the desorber exit are slightly different in the ASPEN and the EES models. However, these differences are merely in definition and do not affect the results for the rest of the cycle. The diagram of the rectifier and surrounding components of interest is shown in Figure 16 below.

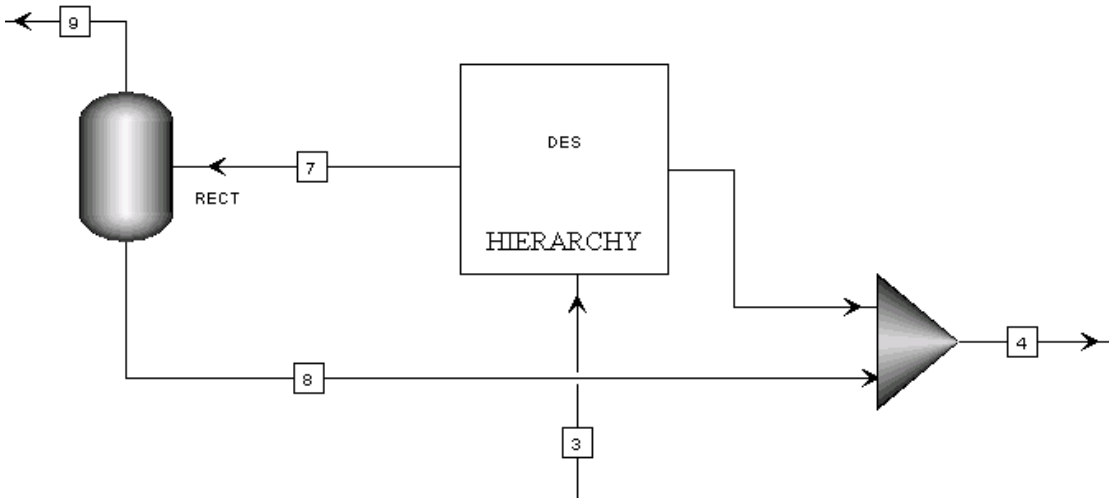

Figure 16: Rectifier model in ASPEN

Vapor/Liquid Heat Exchanger

The vapor/liquid heat exchanger is a component that may or may not be included in the cycle at the designer's discretion. As noted in the state points and assumptions section of this chapter, the vapor/liquid heat exchanger provides a performance benefit in terms of increasing cooling capacity and COP. However, it also adds complexity and initial cost to the design. Initial modeling was done with and without a vapor/liquid heat exchanger, allowing its performance benefit to be

quantified. As it was found that the vapor/liquid heat exchanger increased the cycle COP and cooling capacity by approximately 10%, it was decided that the vapor/liquid heat exchanger was worth including in the cycle design. This is because a premium was placed on cycle performance, and a 10% improvement is clearly worth implementing despite the downsides (increased complexity and initial cost).

The vapor/liquid heat exchanger is in principle very similar to the solution heat exchanger. One side of the heat exchanger is placed between the condenser and the refrigerant valve (creating state 11) and the other side is placed between the evaporator and the absorber (creating state 14). The parameters of the heat exchanger are determined by setting the heat rejected from states 10 to 11 equal to the heat gained from states 13 to 14 and by selecting a pinch temperature between states 10 and 14. The vapor/liquid heat exchanger design is shown in Figure 17 below.

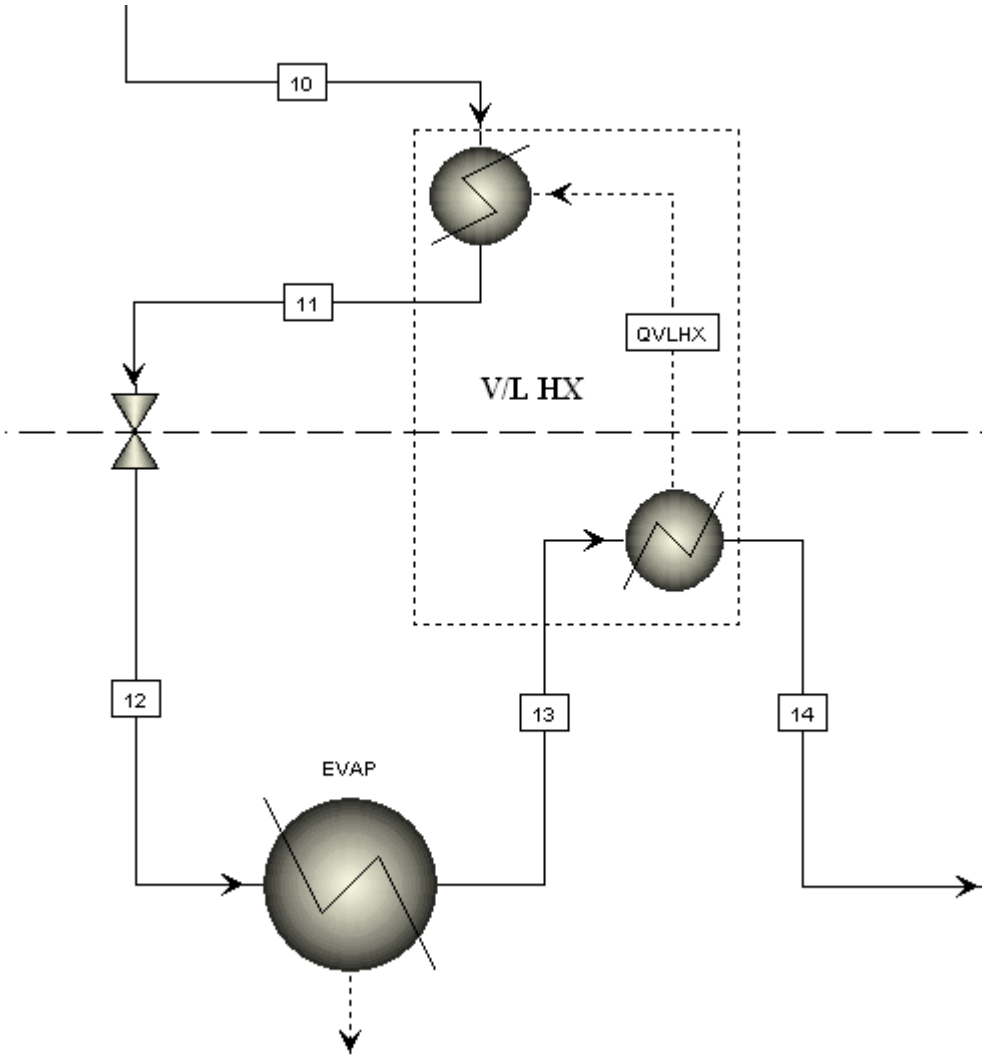

Figure 17: Vapor/liquid heat exchanger model in ASPEN

Adaptation to Desired Inputs

Once the ammonia water working model was created, they were adapted to require desired inputs only. Those inputs are:

- Either quantity of waste heat available or desired cooling load
- Evaporator exit temperature (related to desired cooling temperature)
- Condenser and absorber exit temperatures (related to ambient temperature, or whatever other medium they are rejecting heat to)
- Desorber exit temperature (related to temperature of available waste heat)

- Desired mass percent ammonia at rectifier exit

Each of these inputs defines a pressure, concentration, mass flow rate, or the rectifier load as enumerated below. Either waste heat available or cooling load defines the mass flow rate through the pump. Evaporator exit temperature defines the low pressure. Absorber exit temperature defines the solution concentration at the absorber exit. The condenser exit temperature defines the high pressure. Both of these are related to ambient temperature. The temperature at the liquid exit of the desorber (related to the temperature of the available heat) defines the concentration at the desorber exit. Finally, the desired mass percent ammonia (which was always assumed to be 99%) at the rectifier exit defines the rectifier load.

To accomplish the adaptation to desired inputs in ASPEN, the user must define a design spec, instructing ASPEN to vary the appropriate variable so that desired input variable reaches the desired value. For example, to meet the desired cooling load, instruct ASPEN to vary the total mass flow rate until the desired evaporator duty was met.

Complete Model

The complete model in ASPEN is shown in Figure 18 below. The desorber model was placed in a hierarchy block to reduce clutter.

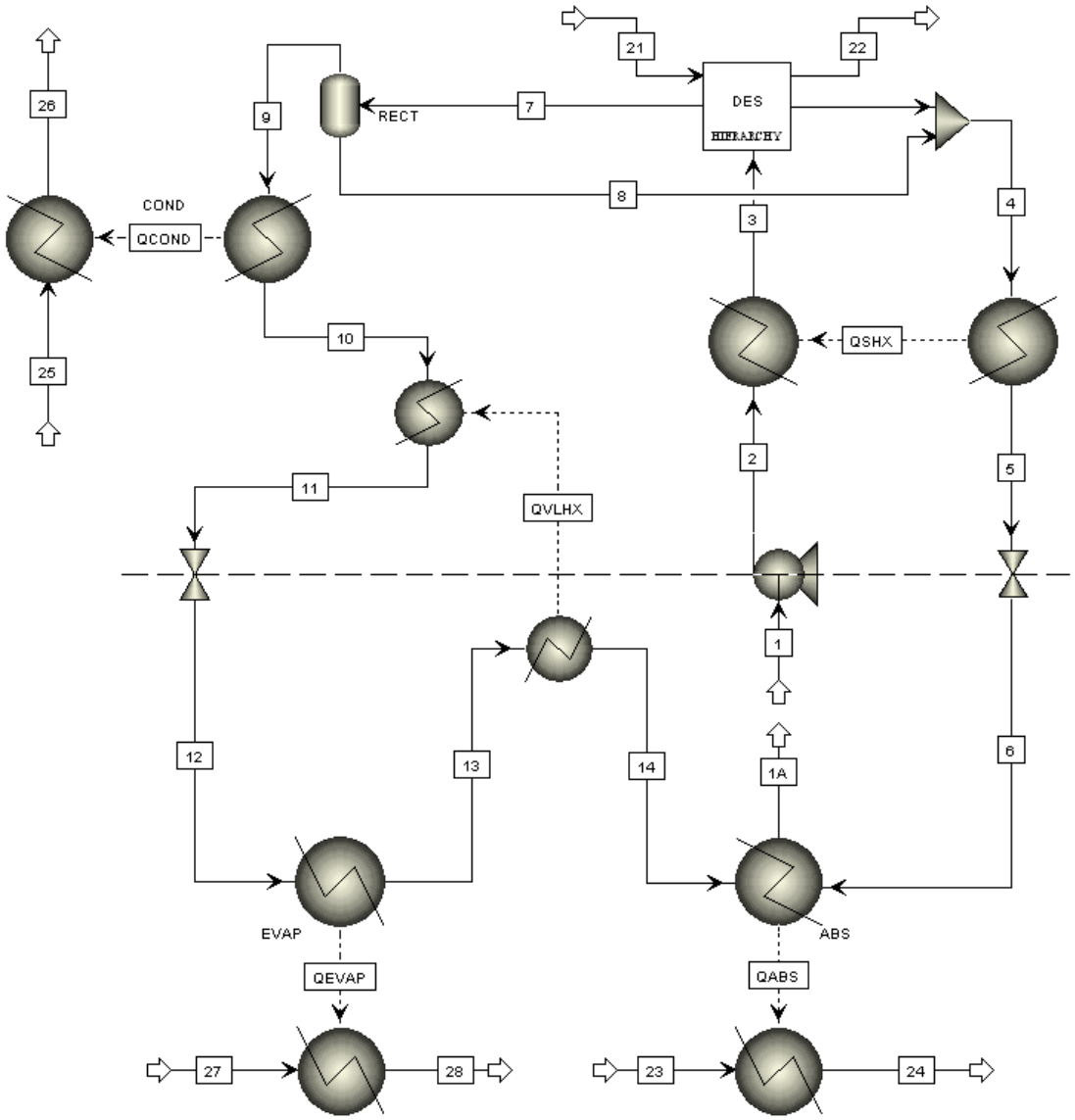

Figure 18: Single effect ammonia/water cycle model in ASPEN

Chapter 5: Absorption Chiller Model Verification

This section is dedicated to assessing the validity of the models, which was a vital step before they are used to produce results. Five checks were performed. Two, a mass balance and an energy conservation verification, were performed to confirm that the models were well formulated and internally consistent. A comparison to EES models for basic cycle parameters (COP, cooling capacity) gave an estimate as to how accurate the models were. A comparison with experimental results confirms that the modeled results agreed with actual performance. Both methods were used because more detail is available for the EES verification, while the experimental verification is more direct. Finally, state-by-state results will be compared against EES predicted results. This final verification more thoroughly reports the results of the ASPEN model and more exhaustively compares them to the EES models.

Mass Balance Verification

As one way of verifying each model, a mass balance verification was performed. As discussed in chapters three and four, it is necessary to include a "break" in the cycle to provide inputs. For all of the models, this break was included in stream 1, between the absorber exit and the pump. A well formulated model will conserve mass throughout the cycle, thus resulting in identical overall and component mass flow rates on either side of the break. In all three cycles, the stream coming out of the absorber was named "1A" and the stream entering the pump was named "1". Table 4, Table 5, and Table 6 show the results of this verification for the single and

double effect water/LiBr and the single effect ammonia/water models. As these results show, each model conserves mass and therefore passes the test.

Table 4: Single effect water/LiBr cycle mass balance verification

MFR (kg/s)	Stream 1	Stream 1A
Total	1.000	1.000
Water	0.426	0.426
LiBr	0.574	0.574

Table 5: Double effect water/LiBr cycle mass balance verification

MFR (kg/s)	Stream 1	Stream 1A
Total	1.000	1.000
Water	0.473	0.473
LiBr	0.527	0.527

Table 6: Single effect ammonia/water cycle mass balance verification

MFR (kg/s)	Stream 1	Stream 1A
Total	1.000	1.000
Ammonia	0.670	0.670
Water	0.330	0.330

Energy Conservation Verification

Additionally, an energy conservation check was performed. This verification is to confirm that the net amount of energy into and out of the cycle is zero. Internal energy transfer is not considered in this verification (for example, the solution heat exchangers, the high pressure condenser-intermediate pressure desorber in the double

effect cycle, and the vapor/liquid heat exchanger in the ammonia/water cycle). Thus, the equation that must be satisfied for each cycle is:

$$E_{in} + E_{out} = 0 \tag{5}$$

This equation is applied to each cycle design for a given design point.

For the single effect cycle water/LiBr design, there are five components that contribute to this equation. The condenser and absorber reject energy out of the cycle, while the evaporator, desorber, and pump add energy to the cycle. However, the pump's contribution is so small that it can be neglected. Thus:

$$|Q_{Cond} + Q_{Abs}| - |Q_{Evap} + Q_{Des}| = 0 \tag{6}$$
$$11.434 + 13.924 - 10.772 - 14.585 = 0$$
$$0 = 0$$

The double effect cycle water/LiBr design has three additional relevant components: and additional pump, condenser, and desorber. As with the single effect cycles, the pumps' contributions are negligible. Also, since heat transferred from the high pressure condenser to the intermediate pressure desorber is internal, it does not contribute. Thus:

$$|Q_{I.\ Cond} + Q_{Abs}| - |Q_{Evap} + Q_{H.Des}| = 0 \tag{7}$$
$$197.70 + 442.15 - 372.49 - 267.36 = 0$$
$$0 = 0$$

Finally, for the single effect cycle ammonia/water design, the contributing components are the same as for the single effect water/LiBr design with the addition of the rectifier, except that the pump contribution is not negligible. Thus:

$$|Q_{Cond} + Q_{Abs} + Q_{Rect}| - |Q_{Evap} + Q_{Des} + W_{Pump}| = 0 \tag{8}$$
$$176.0 + 219.1 + 54.1 - 168.0 - 274.8 - 6.4 = 0$$
$$0 = 0$$

Based on these findings, it is observed that each model is internally consistent with respect to conserving energy throughout the cycle.

Model Accuracy Verification with EES

Having confirmed in the last two sections that the model is internally consistent, it is now necessary to compare the results to another, reputable source of results. Thus, the ASPEN models were compared with the EES models developed by Herold et al. [31]. As was alluded to in section 2 of this thesis, the same assumptions were made in creating the ASPEN models as were used in these EES models to allow for a meaningful comparison.

Single Effect Water/LiBr Cycle

Table 7 details the model verification performed for the single effect water/LiBr cycle. Note that the evaporator heat duty discrepancy is marked as not applicable because its duty was used as an input to the model. The results are very promising; no parameter has more than a 3% error, with many below or near 1%. Those that have errors between two and three percent are all heat duties, which reflects the imperfect property method used in ASPEN.

Double Effect Water/LiBr Cycle

Table 8 details the model verification performed for the double effect water/LiBr cycle. As with the single effect cycle, the evaporator heat duty discrepancy is marked as not applicable because its duty was used as an input to the model. The double effect model's discrepancy is larger than that of the single effect model but still less than 5% for all parameters of interest.

Single Effect Ammonia/Water Cycle

Table 9 details the model verification performed for the single effect cycle. As with the water/LiBr cycles, the evaporator heat duty discrepancy is marked as not applicable because its duty was used as an input to the model. As expected, there is more of a discrepancy with the ammonia/water model than with the water/LiBr, which is no doubt a result of a less applicable property method being used. However, the pressure discrepancies are still very low (around 1%), the heat duty discrepancies are acceptable (all less than 7%), and the COP discrepancy is less than 5%. The concentration errors are notable, but consistent with the findings of the published paper on modeling ammonia/water chillers which also had large discrepancies in predicting concentrations using the Peng-Robinson method [25].

Table 7: Single effect water/LiBr cycle verification with EES

Parameter	Units	EES	ASPEN	Discrepancy
P low	kPa	0.673	0.6715	0.22%
P high	kPa	7.445	7.4606	0.21%
LiBr concentration (strong solution)	%	56.7	57.4	1.23%
LiBr concentration (weak solution)	%	62.5	62.57	0.11%
Q absorber	kW	14.297	13.923	2.62%
Q condenser	kW	11.427	11.432	0.04%
Q desorber	kW	14.952	14.592	2.41%
Q evaporator	kW	10.772	10.772	N/A
COP		0.720	0.738	2.47%

Table 8: Double effect water/LiBr cycle verification with EES

Parameter	Units	EES	ASPEN	Discrepancy
P low	kPa	0.8810	0.8805	0.06%
P middle	kPa	4.1780	4.1776	0.01%
P high	kPa	64.2970	64.3700	0.11%
LiBr concentration (strong solution)	%	52.76	52.72	0.07%
LiBr concentration (weak solution)	%	61.96	61.6	0.57%
Q absorber	kW	435.99	421.25	3.38%
Q cond/des	kW	192.68	189.86	1.46%
Q intermediate pressure condenser	kW	185.61	188.58	1.60%
Q evaporator	kW	354.19	354.37	N/A
Q high pressure desorber	kW	267.39	255.43	4.47%
COP		1.325	1.387	4.74%

Table 9: Single effect ammonia/water cycle verification with EES

Parameter	Units	EES	ASPEN	Discrepancy
P low	kPa	262.9	259.6	1.24%
P high	kPa	1540	1528.0	0.78%
Ammonia concentration (strong solution)	%	38.2	33.0	13.59%
Ammonia concentration (weak solution)	%	28.2	25.9	8.12%
Q absorber	kW	235	219.1	6.77%
Q condenser	kW	173	176.0	1.74%
Q desorber	kW	266	274.8	3.30%
Q evaporator	kW	168	168.0	N/A
COP		0.625	0.598	4.32%

Experimental Verification

To this point, the only external source of comparison for the ASPEN model was EES modeling results. While experimental results are preferable to EES modeling results, suitable experimental data to conduct a thorough comparison is simply not available. Instances of available experimental results are scarce, and when they are available they only give a few results (such as COP and cooling capacity).

This approach is justified because EES is known to have good agreement with experimental results; thus, a model that compares favorably to the EES models will compare favorably to experimental results [23]. However, as a final verification, the ASPEN model will be compared with the limited experimental results available in literature. Unfortunately, only experimental results for water/LiBr chillers were found. This comparison is described below.

The experimental data describes a COP of between 0.73 and 0.76 for a given set of operating conditions. Depending on the assumptions that are used to mimic these conditions, the ASPEN model predicts a COP of between 0.7 and 0.745, for an average discrepancy (0.023, or 3%) less than the range of experimental results (0.030, or 4%). Additionally, the experimental results give a cooling capacity of between 15.8 and 16.6 tons (55.6 to 58.3 kW), similar to the 60.4 kW the model predicts (a discrepancy of 3.4 kW, or 6%).

State Point Results

Finally, a typical set of state points generated by the ASPEN model for each cycle are shown for completeness. For ease of comparison, the mass flow rate was normalized to be 1 kg/s for all three models. Table 10 and Table 11 show the state

points for the single and double effect water/LiBr model, respectively. A discussion of how these results compare to those of EES models follows the tables. The numbered streams correspond to various state points of interest as enumerated in chapter three. Note that for the double effect cycle, low, intermediate and high pressures were abbreviated L., I., and H.

Table 10: Single effect water/LiBr cycle state point results from ASPEN models

	Units	1	2	3	4
From		Absorber	Pump	SHX	Desorber
To		Pump	SHX	Desorber	SHX
Temperature	°C	32.7	32.7	63.8	89.9
Pressure	kPa	0.672	7.461	7.461	7.461
Quality		0.000	0.000	0.000	0.000
MFR	kg/s	1.000	1.000	1.000	0.918
X_{LiBr}		57.4%	57.4%	57.4%	62.6%
	Units	**5**	**6**	**7**	**8**
From		SHX	Valve	Desorber	Condenser
To		Valve	Absorber	Condenser	Valve
Temperature	°C	53.3	43.1	78.4	40.2
Pressure	kPa	7.461	0.672	7.461	7.461
Quality		0.000	0.010	1.000	0.000
MFR	kg/s	0.918	0.918	0.083	0.083
X_{LiBr}		62.6%	62.6%	0.0%	0.0%
	Units	**9**	**10**		
From		Valve	Evaporator		
To		Evaporator	Absorber		
Temperature	°C	1.3	1.3		
Pressure	kPa	0.672	0.672		
Quality		0.070	1.000		
MFR	kg/s	0.083	0.083		
X_{LiBr}		0.0%	0.0%		

Table 11: Double effect water/LiBr cycle state point results from ASPEN models

	Units	1	2	3	4
From		Absorber	L. Pump	I. SHX	I. Desorber
To		L. Pump	I. SHX	I. Desorber	I. SHX
Temperature	°C	29.9	29.9	46.9	74.9
Pressure	kPa	0.881	4.178	4.178	4.178
Quality		0.000	0.000	0.000	0.000
MFR	kg/s	1.000	1.000	1.000	0.856
X_{LiBr}		52.7%	52.7%	52.7%	61.6%
	Units	**5**	**6**	**7**	**8**
From		I. SHX	Valve	I. Desorber	I. Condenser
To		Valve	Absorber	I. Condenser	Valve
Temperature	°C	52.4	45.5	57.7	29.7
Pressure	kPa	4.178	0.881	4.178	4.178
Quality		0.000	0.007	1.000	0.000
MFR	kg/s	0.856	0.856	0.066	0.144
X_{LiBr}		61.6%	61.6%	0.0%	0.0%
	Units	**9**	**10**	**11**	**12**
From		Valve	Evaporator	I. Desorber	I. Pump
To		Evaporator	Absorber	I. Pump	H. SHX
Temperature	°C	5.1	5.1	57.7	57.8
Pressure	kPa	0.881	0.881	4.178	64.370
Quality		0.041	1.000	0.000	0.000
MFR	kg/s	0.144	0.144	0.541	0.541
X_{LiBr}		0.0%	0.0%	52.7%	52.7%

	Units	13	14	15	16
From		H. SHX	H. Desorber	H. SHX	Valve
To		H. Desorber	H. SHX	Valve	I. Desorber
Temperature	°C	91.1	144.8	101.3	77.1
Pressure	kPa	64.370	64.370	64.370	4.178
Quality		0.000	0.000	0.000	0.025
MFR	kg/s	0.541	0.463	0.463	0.463
X_{LiBr}		52.7%	61.6%	61.6%	61.6%
	Units	**17**	**18**	**19**	
From		H. Desorber	H. Condenser	Valve	
To		H. Condenser	Valve	I. Condenser	
Temperature	°C	123.3	87.8	29.7	
Pressure	kPa	64.370	64.370	4.178	
Quality		1.000	0.000	0.100	
MFR	kg/s	0.078	0.078	0.078	
X_{LiBr}		0.0%	0.0%	0.0%	

These results compare favorably to results from EES models [31]. For the single effect water/LiBr cycle, the percent pressure discrepancies for all state points are less than 0.25% and the absolute LiBr concentration discrepancies are less than 1%. The absolute temperature discrepancies are less than 2°C for all state points, with all but two state points having less than 1 degree discrepancy.

For the double effect water/LiBr cycle, the percent pressure discrepancies for all state points are less than 0.15% and the absolute LiBr concentration discrepancies are less than 0.5%. The absolute temperature discrepancies are less than 3°C for all state points, with all but three state points having less than 1 degree discrepancy.

The same was done for the single effect ammonia/water cycle with vapor/liquid heat exchanger, shown in Table 12 below. A discussion of how these results compare to those of EES models follows the table. The numbered streams correspond to various state points of interest as enumerated in chapter four.

Table 12: Single effect ammonia/water cycle state point results from ASPEN models

	Units	1	2	3	4
From		Absorber	Pump	SHX	Desorber
To		Pump	SHX	Desorber	SHX
Temperature	°C	40.0	40.7	112.7	127.1
Pressure	kPa	260	1528	1528	1528
Quality		0.000	0.000	0.023	0.001
Mass Flow	kg/s	1.000	1.000	1.000	0.903
X_{NH3}		33.0%	33.0%	33.0%	25.9%
	Units	**5**	**6**	**7**	**8**
From		SHX	Valve	Desorber	Rectifier
To		Valve	Absorber	Rectifier	Desorber
Temperature	°C	40.7	40.9	114.0	76.4
Pressure	kPa	1528	260	1528	1528
Quality		0.000	0.000	1.000	0.000
Mass Flow	kg/s	0.903	0.903	0.112	0.015
X_{NH3}		25.9%	25.9%	92.7%	51.3%

	Units	9	10	11	12
From		Rectifier	Condenser	V/L HX	Valve
To		Condenser	V/L HX	Valve	Evaporator
Temperature	°C	76.4	40.0	-12.5	-12.2
Pressure	kPa	1528	1528	1528	260
Quality		1.000	0.000	0.000	0.000
Mass Flow	kg/s	0.097	0.097	0.097	0.097
X_{NH3}		99.0%	99.0%	99.0%	99.0%
	Units	**13**	**14**		
From		Evaporator	V/L HX		
To		V/L HX	Absorber		
Temperature	°C	-10.0	35.0		
Pressure	kPa	260	260		
Quality		0.893	0.999		
Mass Flow	kg/s	0.097	0.097		
X_{NH3}		99.0%	99.0%		

These results compare reasonably well to the results from the EES models [31]. The percent pressure discrepancies for all state points are around 1%. The ammonia concentrations have around or less than 5% absolute discrepancy. The temperature discrepancies warrant further discussion. For all state points except 3, 7, and 8, the temperature errors are less than 3°C, with many below 1°C. State point 3 has a discrepancy of around 5°C, and state point 7 has a discrepancy of around 10°C. State point 8 does not agree with EES because it was defined differently than in the EES models.

Chapter 6: Gas Turbine Modeling and Integration

Background

Motivation

With the absorption chiller models verified, the next step was to identify a waste heat source to use as a driver. Oil and gas plants have a number of waste heat sources, such as hot exhaust gasses (gas turbine or boiler exhausts), hot streams that need to be cooled, and steam [33]. Although other waste heat sources are viable, plant operators are unable to alter any of the plant cycle itself. Thus, this study will only consider gas turbine exhaust, which is viable because it is high temperature (several hundred degrees Celsius, depending on the model), available in large quantities (on the order of megawatts), and has high availability.

Gas Turbine Selection and Specifications

Next, a specific gas turbine model was selected to determine the temperature and quantity of waste heat available. Because it is commonly used in APCI-design LNG plants, the GE MS5001 model was selected. Usually, two or three MS5001s are used in APCI-design plants. The specifications for the MS5001 are listed below:

Table 13: GE MS5001 Specifications [33, 34]

Specification	Value	Units
ISO Rated Power	24.6	MW
Firing Temperature	943	°C
Air Flow Rate	118	kg/s
Exhaust Temperature	484	°C
Heat Rate	12,808	kJ/kW-hr
Efficiency	28.1	%
Pressure Ratio	10.5	

Modeling and Verification

It was necessary to find or generate a model for the selected gas turbine in ASPEN Plus. Since a colleague had already created such a model and there was no need to repeat his work, his model was used. His modeling process was detailed in a paper currently under consideration for journal publication [33]. It is also summarized in the following section.

Assumptions and Component Breakdown

Firstly, a property method had to be chosen. The Peng-Robinson-Boston-Mathias method (abbreviated PR-BM in ASPEN) was selected because it is recommended for gaseous substances at high temperatures [8].

Next, the gas turbine design was decomposed into a compressor, a combustion chamber, and a turbine. This is convenient because each of these has an exact analogue in ASPEN. The compressor model has ambient air as an inlet; the mass flow rate at the compressor inlet was selected to be equal to the manufacturer given value of 118 kg/s for the gas turbine inlet and was kept constant. The outlet, which goes to

the combustion chamber, is determined by assuming zero pressure drop at the compressor inlet, a compressor ratio of 10.5, and an isentropic efficiency of 83%.

The combustion chamber has two inlets, the compressor outlet and the fuel. The fuel was assumed to be pure methane at 15°C and 1300 kPa. At full load its mass flow rate is set to match the manufacturer-specified firing temperature. Once the "full load" fuel rate is set (in this case, 6,230 kg/hr), part loading is simulated by adjusting the fuel mass flow rate. The chamber is assumed to have zero pressure drop and zero heat duty (i.e. the fuel is the sole contributor to heat addition in the combustion chamber). The reactor model minimizes Gibbs Free Energy to predict the products.

The reactor products exit the combustion chamber and enter the turbine. The turbine's isentropic efficiency is assumed to be 85%, the pressure ratio is taken to be 10.5, and the pressure drop at the gas turbine exit is assumed to be zero. The turbine exhaust is synonymous with the exhaust of the gas turbine.

Finally, the gas turbine exhaust goes to a heat exchanger block, which simulates the removal of waste heat. Zero pressure drop was assumed, and the exit temperature of the block (equivalent to the lowest temperature was heat that is useful) was selected to be 200°C. This is because condensation issues might arise at temperatures lower than 200°C, thus, 200°C is a conservative approximation.

The complete model PFD in ASPEN can be found at the end of this section.

State Points and Streams

For reference, the model's streams are summarized in Table 14 below. The first five streams are material streams and correspond to the five state points of interest. The next two are work streams, representing quantities of work of interest in

the gas turbine. The "TRB" prefix is used because stream names cannot be duplicated. If a simple numbering system were used, this would create a problem when the turbine model and the chiller models are joined since the chiller streams are also numbered 1, 2, 3, etc.

Table 14: Gas turbine model streams

Stream	Type	Description
TRB1	Material	Inlet air to compressor
Fuel	Material	Inlet fuel to combustion chamber
TRB2	Material	Compressor outlet
TRB3	Material	Combustion chamber outlet
TRB4	Material	Turbine exhaust
WBACK	Work	Back work
WNET	Work	Net mechanical output of gas turbine

Verification

The study that details the modeling process for this gas turbine also details the model verifications conducted, which for brevity they will not be included. The MS5001 was compared to experimental data and was found to have less that 5% error. The model was found to be conservative in predicting results [33].

Model PFD

The complete model process flow diagram is shown in the figure below.

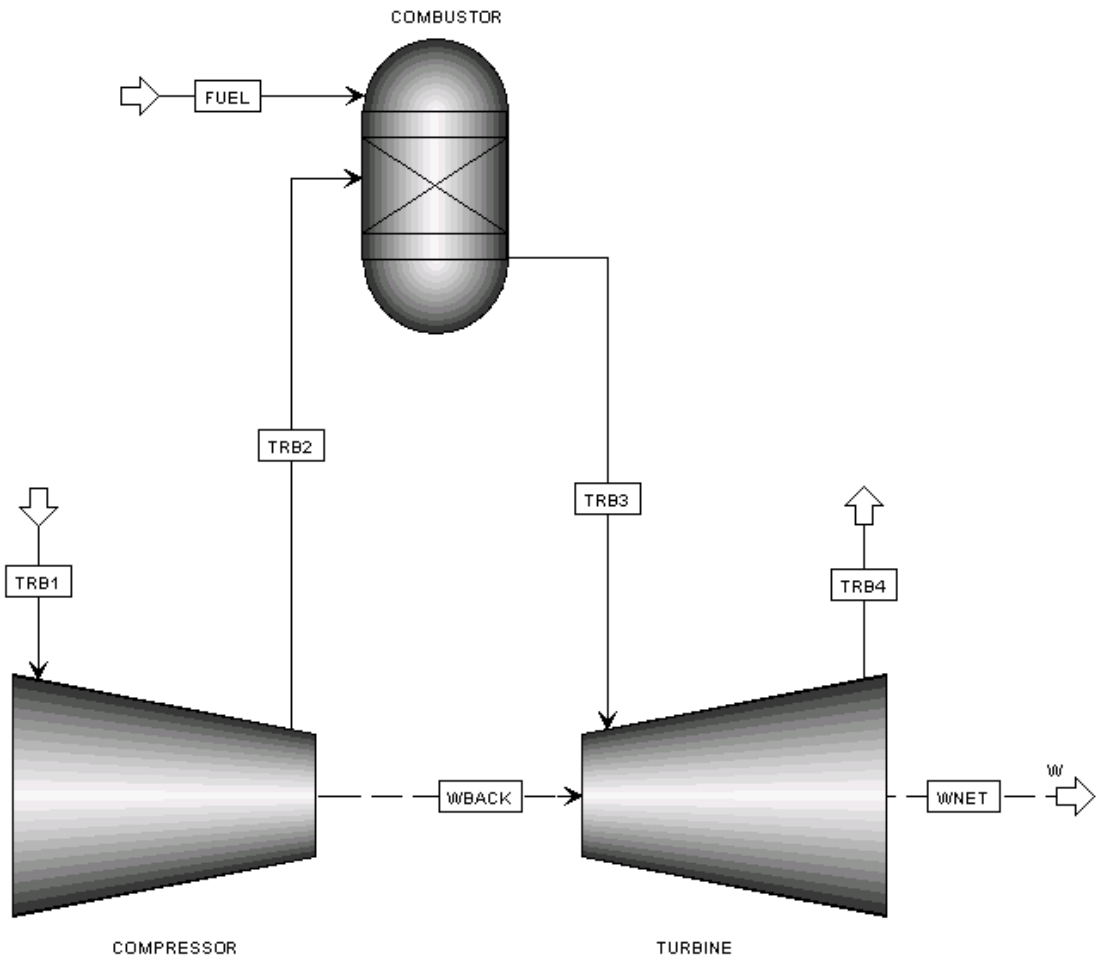

Figure 19: Gas turbine model in ASPEN

Integration with Chiller Models

The last step was to integrate the various chiller designs into the gas turbine model. Three new models were created, one each with the gas turbine and each of the chiller designs. In each model, the gas turbine exhaust gasses were set up to exchange heat directly with the desorber of the chiller. The gas turbine exhaust after this heat exchange was set to 200 °, corresponding to the "usable waste heat temperature" described earlier in this chapter.

There are two parameters that were considered for the interface between the gas turbine and the chiller: the amount of waste heat available and the temperature of

the waste heat. To accomplish the first interface, the mass flow rate through the main pump of the chiller was varied to match the desorber duty to the amount of waste heat available. Effectively, this sizes the chiller to match the amount of waste heat available. To address the temperature interface, the highest desorber temperature is 180°C (used in the double effect water/LiBr chiller) and the lowest usable temperature waste heat from the turbine exhaust is 200°C. This 20°C temperature difference was considered large enough that temperature is not a concern. The single effect cycles use much lower desorber temperatures; thus, temperature is even less of a concern for them. However, an analysis on the demand of the heat exchanger between the gas turbine exhaust and the desorber can be found in chapter 7.

Model Process Flow Diagram

The complete gas turbine/chiller model process flow diagram is shown in Figure 20 for the single effect water/LiBr cycle. Similar models were created for the other two chiller designs, and are not shown because they are very similar.

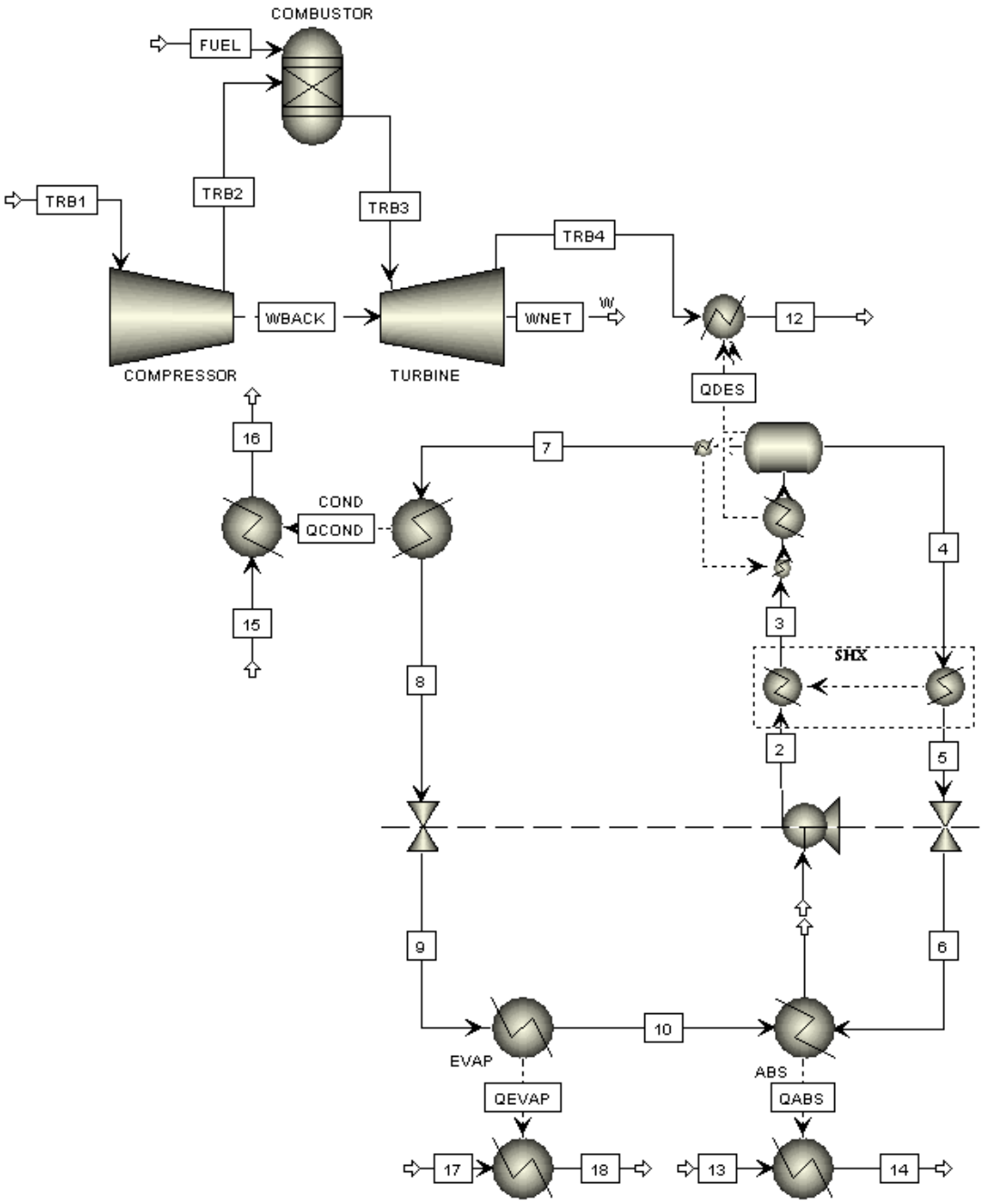

Figure 20: Gas turbine and single effect water/LiBr integrated model in ASPEN

Chapter 7: Results

With the chiller and gas turbine models completed, results can now be obtained. Three distinct studies were conducted. Firstly, parametric studies on part loading, evaporator temperature, and ambient conditions were performed to evaluate the effect on performance on these parameters. Secondly, a study was conducted to select the best of the three designs for the application of interest. Finally, a study was performed to determine the performance of this best design throughout the course of a year based on site weather conditions.

Parametric Studies

The first set of results obtained from the models was a set of parametric studies. These studies revealed the effects of varying parameters of interest on system performance. The parameters of interest selected were turbine part loading, evaporator temperature and ambient conditions.

Assumptions and "Default Values"

To begin, a set of "default values" was selected. These values were held constant, except for the parameter of interest being varied, allowing parameters of interest to be isolated. It also allowed for the cycle to have realistic or conservative operating conditions where applicable. The default values are shown in Table 15 and Table 16. They are also discussed following the tables. The six parameters in these two tables are used to define the "base" operating conditions for each cycle.

Table 15: Water/LiBr chiller parametric study default values

Parameter	Value	Units
Turbine Part Load	100	%
Evaporator Temperature	5	°C
Seawater Temperature	35	°C
Seawater ΔT	5	K
Useful Heat Temperature	200	°C
Single Effect Desorber Temperature	95	°C
Double Effect Desorber Temperature	180	°C

Table 16: Ammonia chiller parametric study default values

Parameter	Value	Units
Turbine Part Load	100	%
Evaporator Temperature	-10	°C
Seawater Temperature	35	°C
Seawater ΔT	5	K
Useful Heat Temperature	200	°C
Desorber Temperature	125	°C

Firstly, for all cycles, it was decided that the turbine was set to full load by default. The parametric study regarding part loading addresses other loading conditions. Secondly, a representative evaporator temperature was selected for each cycle. For the water/LiBr cycles, 5°C was selected as a conservative value (at a lower temperature, operating issues with the solution begin to arise, and COP increases with evaporator temperature). For ammonia/water, -10°C was selected because ammonia/water chillers tend to be used at lower evaporator temperatures. The seawater temperature for all chillers was conservatively selected to be 35°C, the

highest seawater temperature in Abu Dhabi. This is a conservative value because COP increases with decreasing seawater temperature as it is used as a heat sink for the absorber and condenser in the cycle. The ΔT between the seawater temperature and the absorber and condenser temperatures was selected to be a representative 5 K. The "useful heat temperature"- the temperature which the gas turbine exhaust can be cooled to - was selected to be 200°C. This was because cooling the exhaust below this temperature can result in condensation issues. Finally, the respective desorber temperatures for each cycle were chosen as representative operating values.

Part Load Operation

The first parametric study conducted was that of varying the part load of the gas turbine. This was an important study because in realistic operation, the gas turbine will not always be operating at 100% load and because at different loading conditions the quantity of waste heat will vary. This study ascertained the relationship between part loading and gas turbine efficiency, as well as the relationship between part load and amount of waste heat available.

Part loading is accomplished by varying the fuel mass flow rate in the turbine linearly; in other words, 80% part load is accomplished by lowering the fuel mass flow rate by 80% of the full load value. Thus, the fuel mass flow rate was diminished incrementally starting at 100% until the model started to have problems converging. The results are shown below in Figure 21 and later in Figure 22.

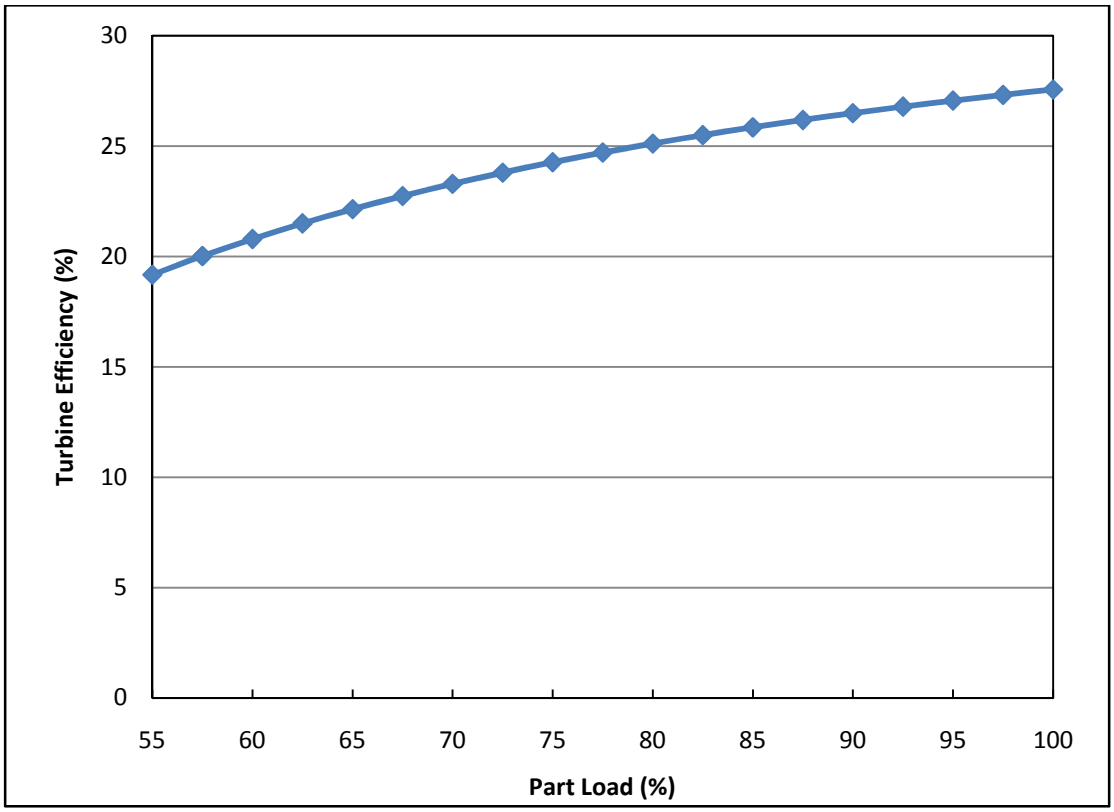

Figure 21: MS 5001 part load efficiency as predicted by ASPEN model

Figure 21 show the relationship between part load and the efficiency of the gas turbine from 55% to 100%. Results are only shown down to 55% part load because at lower values, the ASPEN model became unreliable and had trouble converging. Several things are notable about these results. The 100% part load result is nearly identical to the manufacturer-specified 28.1%, indicative of a well-constructed model. Also, while gas turbine efficiency decreases with part loading, it does not do so drastically. Even at 2/3 load, the turbine's efficiency is only 5% less than at full load.

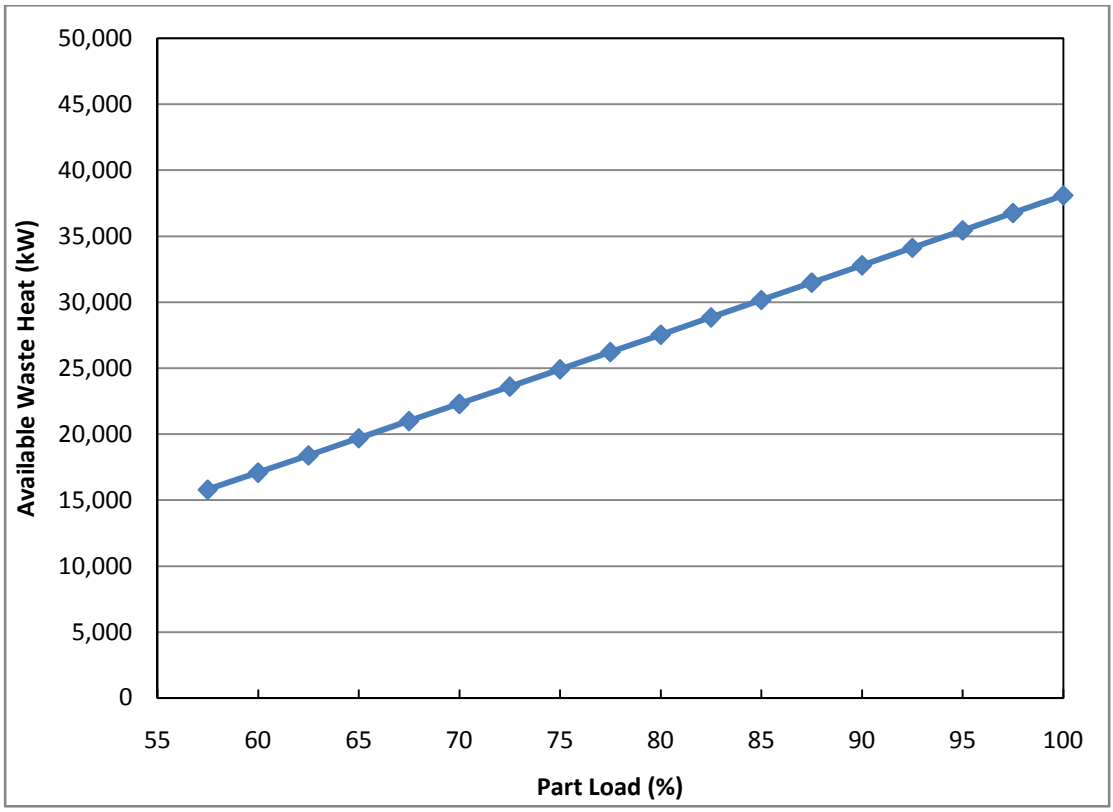

Figure 22: Waste heat available as a function of part loading, GE MS 5001

Figure 22 shows the relationship between part loading and available waste heat. What is notable is that the relationship appears to be nearly linear. Varying part load has two effects on waste heat available. First, the total energy input to the gas turbine is being altered, since the fuel input is being reduced to accomplish part loading. Secondly, turbine efficiency is a function of part load, as demonstrated in Figure 21. This means that the percent of the total energy input into the turbine that becomes waste heat changes. However, since the effect of part loading on efficiency is not significant, approximately the same percentage of the energy entering the cycle becomes waste heat. Thus, waste heat available is nearly directly related to amount of fuel input, which is directly related to part load, explaining the nearly linear relationship between available waste heat and part loading.

Evaporator Temperature

The next parameter of interest is evaporator temperature. This is an important parameter to consider because it has a significant effect on chiller performance, as a higher evaporator temperature means a higher COP. The evaporator temperature is a set value that is dictated by the desired cooling temperature, but since a variety of cooling temperatures are needed in an LNG plant, it is important to consider a variety of evaporator temperatures.

For the two water/LiBr cycles, the range of temperatures investigated started at the default value of 5°C and proceeded upward. Likewise, for the ammonia/water cycle, the range of temperatures investigated started at the default value of -10°C. Though it was alluded to earlier in this chapter, it is worth noting that the range of evaporator temperatures of interest for the ammonia/water cycle is lower because ammonia/water does not face freezing or crystallization issues below 5°C, while water/LiBr begins to. In other words, if an evaporator temperature is required to be below 2-5°C, ammonia/water is the only chiller option.

Results of the parametric study are shown over the next few pages in Figure 23, Figure 24, and Figure 25.

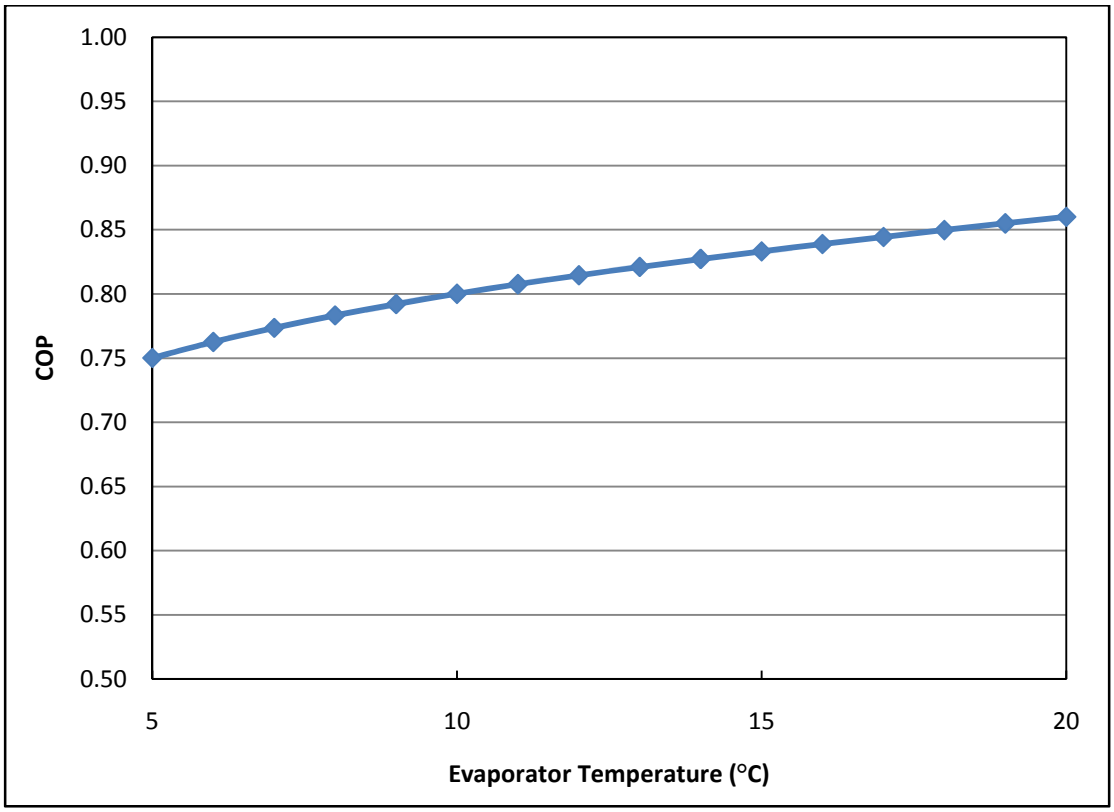

Figure 23: Effect of evaporator temperature on single effect water/LiBr chiller COP as predicted by ASPEN model

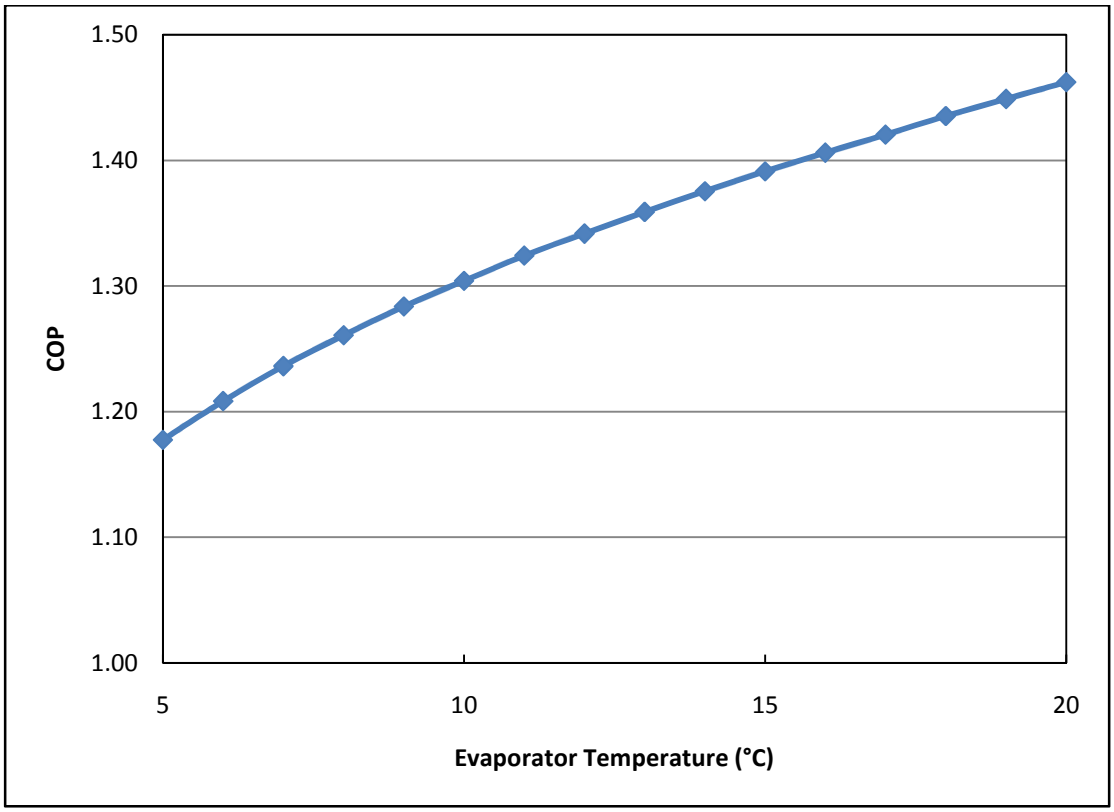

Figure 24: Effect of evaporator temperature on double effect water/LiBr chiller COP as predicted by ASPEN model

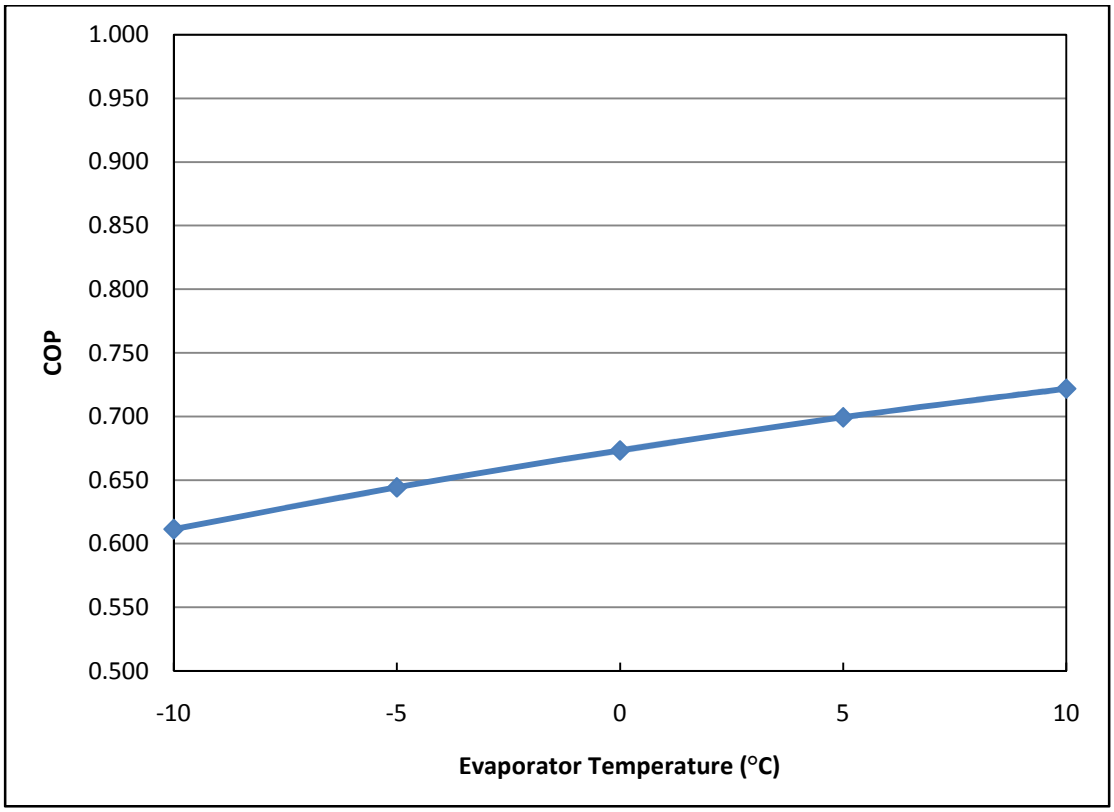

Figure 25: Effect of evaporator temperature on single effect ammonia/water chiller COP as predicted by ASPEN model

The COP of each model increases with increasing evaporator temperature, which is not surprising. The meaningful results come from comparing the trends of each model. First of all, the double effect cycle seems to be the most sensitive to evaporator temperature. Secondly, when comparing the two single effect cycles at the same evaporator temperatures, the water/LiBr chiller's COP is 7% higher, despite having a lower desorber temperature.

Ambient Conditions

The final parameter of interest is ambient conditions. Ambient conditions change throughout the year, and it is important to understand what the effect on performance will be. Two components of chillers reject heat to an ambient sink (in

the case of LNG plants, seawater), the absorber and the condenser. Thus, seawater temperature affects absorber and condenser temperature. Seawater temperature was varied from the most conservative value of 35°C down as low as the models were able to converge. The results of these studies are shown in Figure 26, Figure 27, and Figure 28.

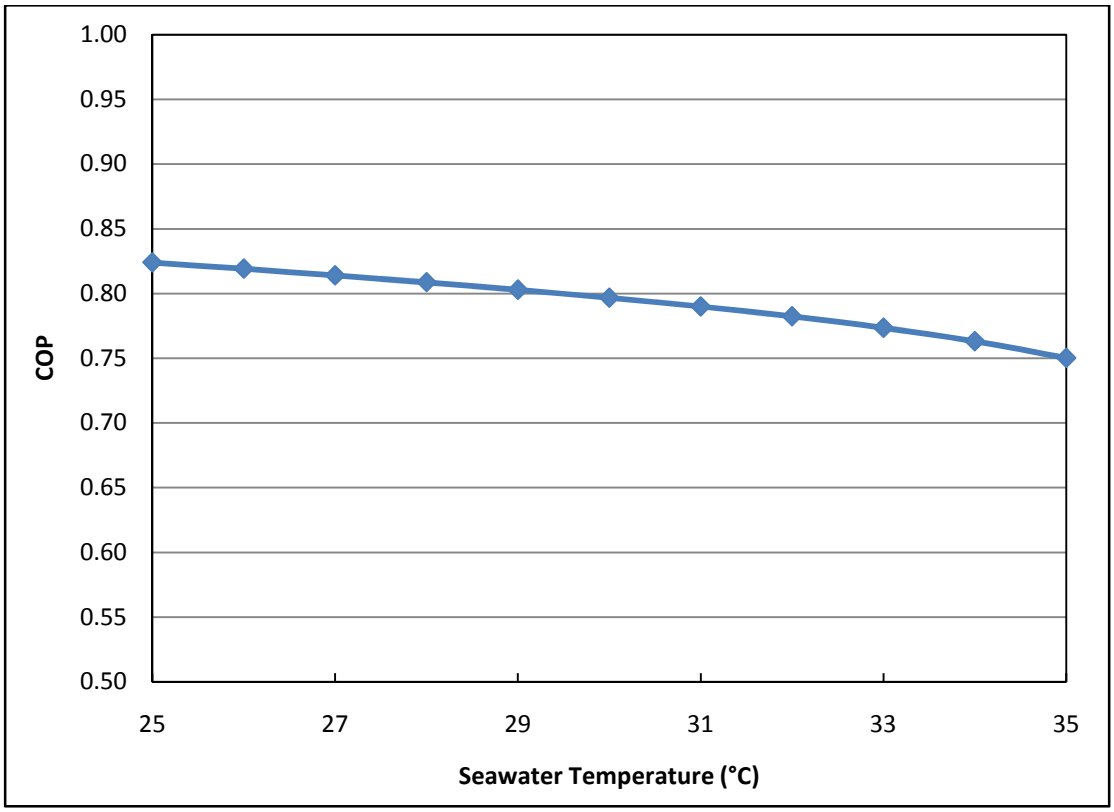

Figure 26: Effect of ambient conditions on single effect water/LiBr chiller COP as predicted by ASPEN model

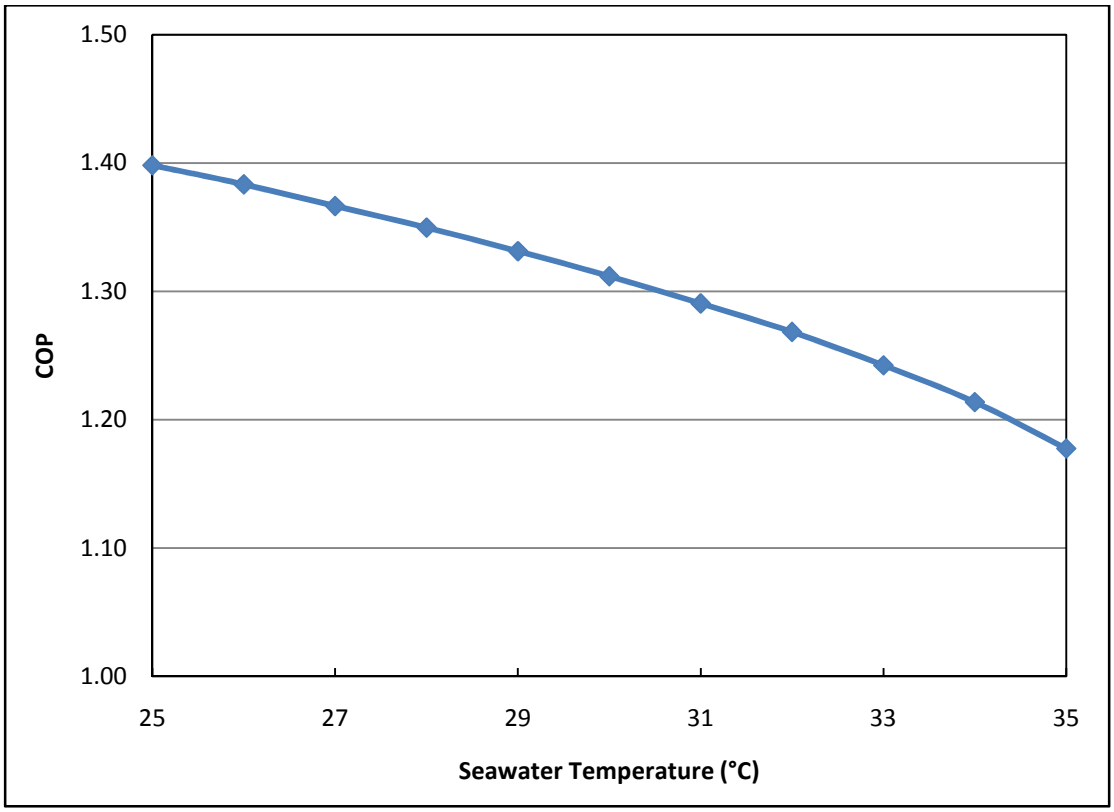

Figure 27: Effect of ambient conditions on double effect water/LiBr chiller COP as predicted by ASPEN model

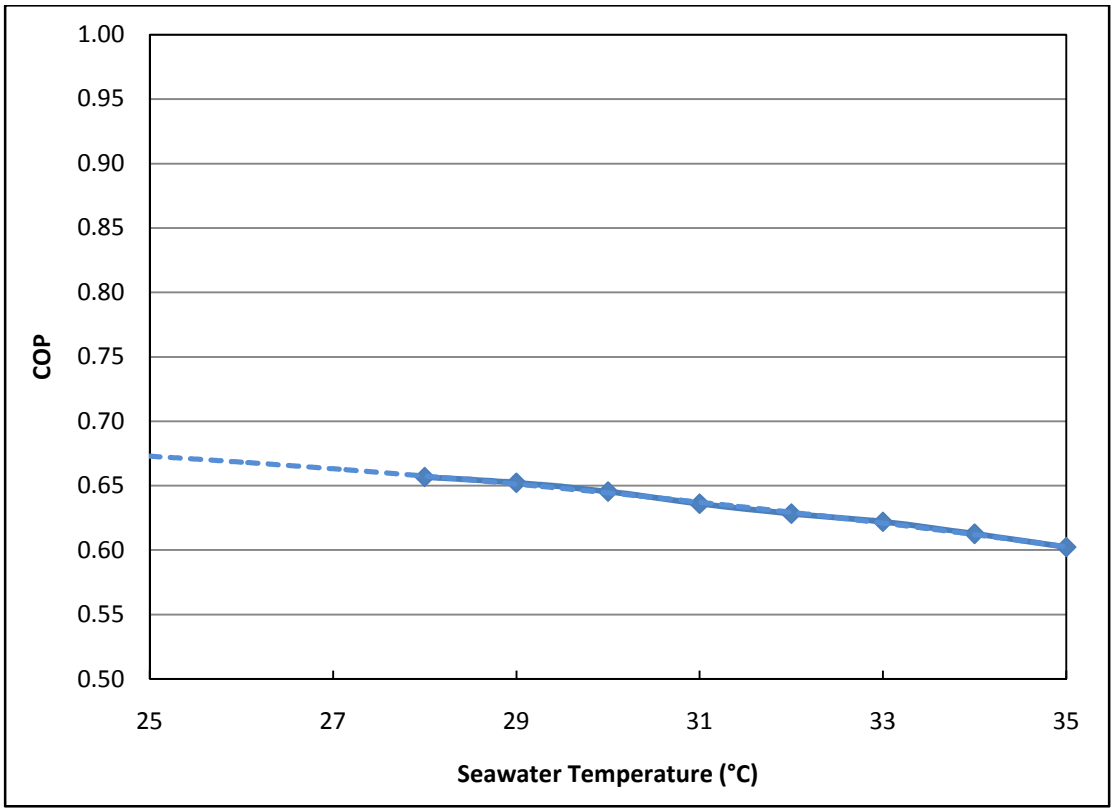

Figure 28: Effect of ambient conditions on single effect ammonia/water chiller COP as predicted by ASPEN model

All three chiller designs show that increasing seawater temperature reduces performance. As in the previous study, the double effect cycle is the most sensitive. Note that the ammonia/water model had trouble converging below 28°C, thus the dotted line shows extrapolated values using a second order curve fit.

Sensitivity Studies

Pressure Drop

To this point, absorption chiller modeling was conducted assuming no pressure drop throughout the system. This approach was justified by the fact that pressure drop does not significantly affect cycle COP. However, this study quantifies the effects of including pressure drop.

A pressure drop resulting in a temperature difference of both 1 K and 2 K in each phase-change device was considered. All other system operating conditions were set to the default values described in Table 15. Modeling a 1 K pressure drop affects the COP of cycle by 0.013, or 1.7%. The 2 K pressure drop affects the COP of the single effect water/LiBr cycle by 0.028, or 3.7%. These results are summarized in Table 17.

Table 17: Sensitivity to pressure drop

Pressure Drop	COP	% Difference in COP Compared to Base Case
None	0.750	0.00%
1 K	0.737	-1.73%
2 K	0.722	-3.73%

This analysis confirms that, while including pressure drop reduces the system COP, the effect is small.

Approach Temperature

Another key assumption made in modeling was the difference in temperature in the absorber and condenser. This study explores the sensitivity to this assumption. The approach temperature of each component was varied independently from 1 K to 8 K. All other system operating conditions were set to the default values described in Table 15. The results are shown below in Table 18 and Table 19.

Table 18: Sensitivity to condenser approach temperature

Approach Temperature (K)	COP	% Difference in COP Compared to Base Case
1	0.780	4.09%
2	0.774	3.20%
3	0.767	2.26%
4	0.759	1.17%
5	0.750	0.00%
6	0.740	-1.32%
7	0.728	-2.86%
8	0.715	-4.66%

Table 19: Sensitivity to absorber approach temperature

Approach Temperature (K)	COP	% Difference in COP Compared to Base Case
1	0.777	3.61%
2	0.771	2.83%
3	0.765	2.01%
4	0.758	1.09%
5	0.750	0.00%
6	0.741	-1.15%
7	0.731	-2.56%
8	0.718	-4.21%

These results guide the designer where to invest resources. Smaller approach temperatures mean better cycle performance, but require more expensive and larger heat exchangers. Additionally, it is evident that an improvement in approach temperature in the condenser will mean a greater improvement in COP, thus, more resources should be spent improving the condenser than the absorber.

Performance Comparison

With the results of the parametric studies in hand, the performance of the three respective chiller designs and the two respective working fluid pairs were compared. In the evaporator temperature study, the single effect water/LiBr cycle outperformed the single effect ammonia/water cycle despite operating at a lower desorber temperature. The very large caveat to this statement is that water/LiBr cannot be used for evaporator temperatures below 2-5°C; thus, the overall conclusion is that for evaporator temperatures above 2-5°C where water/LiBr can be used it is preferable, where it cannot be used, ammonia/water must be.

As expected, double effect cycles outperform single effect cycles for instances where the available waste heat temperature is high, which is the case for gas turbine exhaust. However, the double effect cycle is at an inherent advantage because its high end operating temperature is significantly higher than either single effect cycle. Thus, according to Carnot efficiency, it will naturally outperform either single effect cycle. What if condensation was not an issue and the waste heat source was useful down to whatever temperature the desorber temperature dictated, would the double effect cycle still be preferable?

This study seeks to answer that question. In an attempt to compare all three cycles on an equal basis, the usable waste heat temperature was lowered to the point where the ΔT between it and the desorber temperature was the same for each cycle. This ΔT was chosen to be 20 K, allowing the double effect cycle temperatures were kept unchanged (200°C usable waste heat temperature, 180°C desorber temperature). The usable waste heat temperature for the single effect ammonia/water cycle was

lowered to 145°C (compare to 125°C desorber temperature) and the usable waste heat temperature for the single effect water/LiBr cycle was lowered to 115°C (compare to 95°C desorber temperature). The results of this study are shown in Figure 29 below.

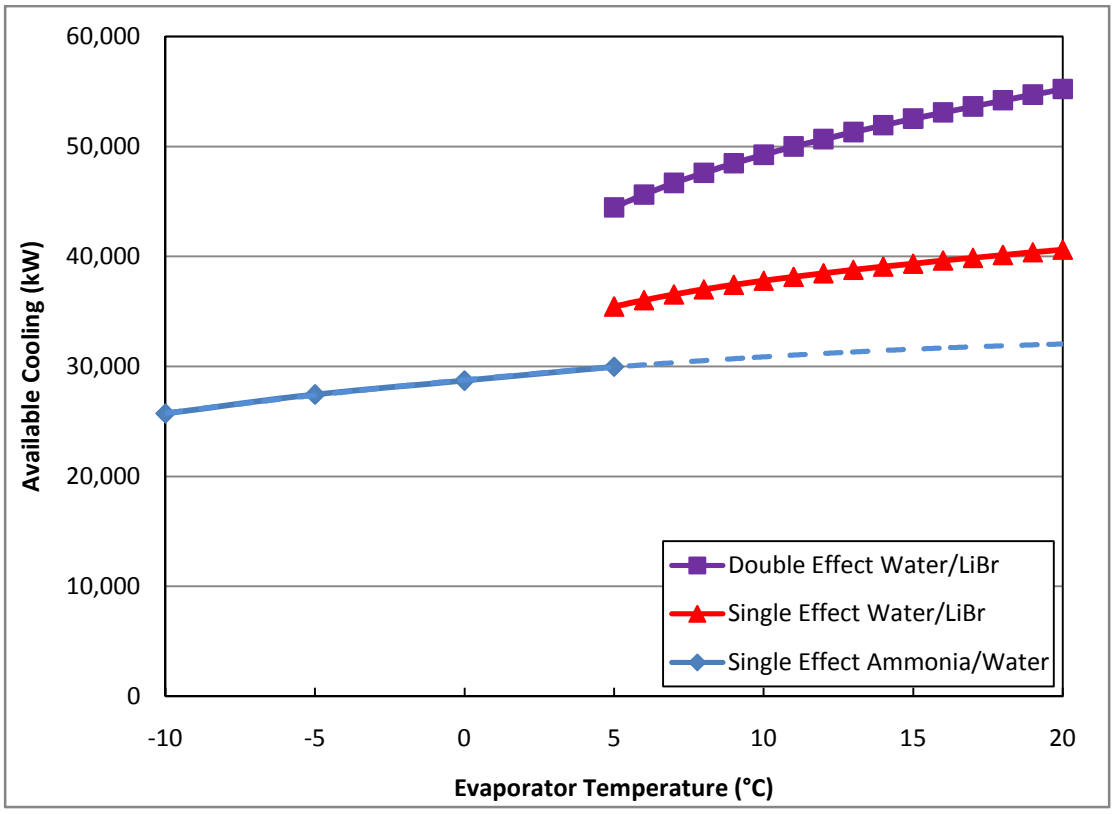

Figure 29: Comparison of cooling capacities of chiller designs at various evaporator temperatures

Note that, due to convergence issue, the dotted line shows extrapolated results for the ammonia/water cycle based on a second-order curve fit. By this means of comparison, the performance of the single effect cycles are, as expected, comparatively improved, but still the double effect cycle is clearly better.

The following conclusions are drawn from the analysis in this section:

- For high temperature waste heat, double effect designs provide more cooling than single effect designs, even in the theoretical case where waste heat is useful down to whatever temperature desired

- Water/LiBr outperforms ammonia/water in terms of COP, with the caveat that it cannot be used for evaporator temperatures below 2-5°C

Since there is ample need for cooling at temperatures above 5°C, for this particular application, a double effect water/LiBr chiller is the best design.

Seasonal Performance

The final study that was conducted was to take the best design (double effect water/LiBr, as chosen in the previous section) and predict its performance when coupled with the selected gas turbine, the MS5001 (see the gas turbine chapter) throughout the course of a year. The two effects that changing ambient conditions have is changing air temperature, which affects the inlet temperature of the gas turbine, and changing seawater temperature, which affects the absorber and condenser temperatures.

Thus, weather data was acquired for the site in question. Hourly weather data for Abu Dhabi was obtained from EnergyPlus [35]. A histogram of the air temperatures throughout a year in Abu Dhabi is shown in Figure 30.

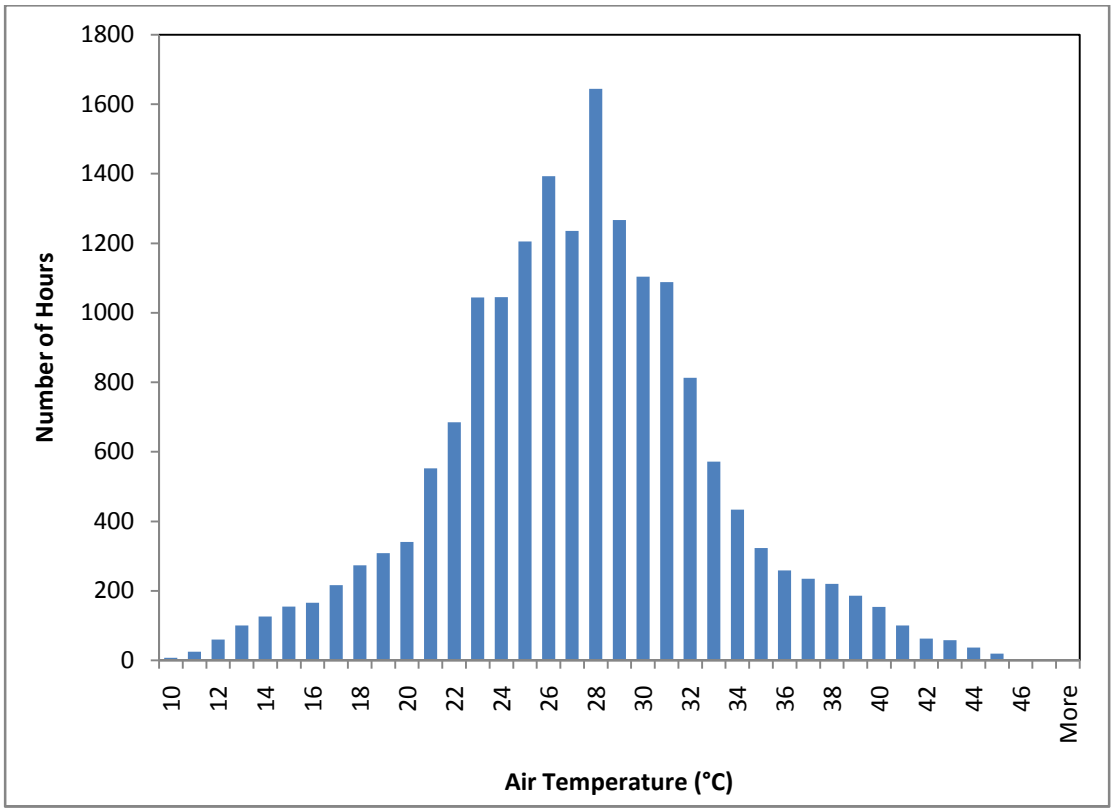

Figure 30: Abu Dhabi air temperatures throughout the year in 1K bins [35]

Seawater temperature also varies seasonally, but hourly weather data is not available for it. However, there is a strong relationship between seawater and air temperature. This relationship was approximated, which required more information. It was known that the minimum seawater temperature in Abu Dhabi is approximately 19°C and the maximum is approximately 35°C. Given that the yearly average air temperature has to be the same as the yearly average seawater temperature, a linear fit was constructed, giving the following relationship (both temperatures in °C):

$$T_{Air} = 2.35 * T_{Seawater} - 35.8 \quad (9)$$

To accomplish the seasonal study, air temperature was varied at 1K increments to match the temperature bins shown in the histogram. A calculator block used the relationship between air temperature and seawater temperature to vary

seawater temperature automatically with air temperature. The evaporator temperature was conservatively selected to be 5°C. Results at each temperature bin were acquired, and were multiplied by the number of hours per year that are within that temperature bin to give the total waste heat and cooling available at each bin. Totaling the results for all temperature bins gives the total annual waste heat and cooling available for the year. These results are shown below in Table 20.

Table 20: Results of seasonal study

T Bin (°C)	Hours	Waste Heat (MWh)	Cooling (MWh)	*T* Bin (°C)	Hours	Waste Heat (MWh)	Cooling (MWh)
9.5	7	228	339	28.5	448	15,794	22,453
10.5	25	819	1,214	29.5	423	14,971	21,203
11.5	60	1,974	2,920	30.5	398	14,142	19,945
12.5	100	3,303	4,876	31.5	380	13,555	19,031
13.5	126	4,180	6,157	32.5	333	11,925	16,659
14.5	155	5,163	7,591	33.5	288	10,353	14,387
15.5	166	5,553	8,147	34.5	298	10,754	14,857
16.5	216	7,255	10,625	35.5	258	9,346	12,830
17.5	273	9,208	13,458	36.5	235	8,546	11,651
18.5	308	10,431	15,216	37.5	220	8,031	10,868
19.5	302	10,270	14,952	38.5	186	6,815	9,149
20.5	363	12,394	18,008	39.5	154	5,664	7,538
21.5	358	12,273	17,795	40.5	100	3,692	4,867
22.5	445	15,318	22,159	41.5	63	2,335	3,047
23.5	361	12,476	18,005	42.5	58	2,157	2,785
24.5	395	13,706	19,730	43.5	37	1,381	1,762
25.5	348	12,124	17,404	44.5	19	712	897
26.5	399	13,956	19,974	45.5	4	150	187
27.5	448	15,732	22,444	46.5	3	113	139
				Total	8760	306,799	**435,267**

This study predicts that a double effect water/LiBr chiller driven by an MS5001 gas turbine is capable of producing 435 GWh of cooling annually, for an average of 49.7 MW. This amount of cooling available is equivalent to 43% of the cooling load of the propane cycle of an APCI-design LNG plant, or 27% of the total cooling load of the plant [36]. These results are summarized in the following table.

Table 21: Predicted available cooling with absorption chillers compared to total cooling demand of APCI-design LNG plant

	Cooling Available with Chillers	Cooling Required	Percent of Demand Met with Chillers
Propane Cycle	49.7 MW	115.5 MW	43.0%
Entire Plant	49.7 MW	183.1 MW	27.1%

Heat Exchanger Demand

Lastly, the demand on the heat exchanger between the gas turbine exhaust and the desorber was considered. To do so, the following formula was used:

$$\mathrm{UA} = \frac{\mathrm{Q}}{\mathrm{LMTD}} \tag{10}$$

UA represents the demand on the heat exchanger. The amount of heat transferred, Q, is known. LMTD is a function of cycle temperatures which are also known, shown in the following equation.

$$\mathrm{LMTD} = \frac{\left(T_{Air,In} - T_{Solution,Out}\right) - \left(T_{Air,Out} - T_{Solution,In}\right)}{\ln\left(\frac{\left(T_{Air,In} - T_{Solution,Out}\right)}{\left(T_{Air,Out} - T_{Solution,In}\right)}\right)} \tag{11}$$

Based on this formula LMTD was calculated to be 164 K, which gave a required UA of 230 kW/K. The UA value is large as due more to the enormous

amount of heat that needs to be transferred than the temperature requirements. Even if the inlet air temperature was around 900°C (on the order of that found in a direct-fired chiller), the UA requirement would still be 133 kW/K. Thus, the heat exchanger would require a UA value 1.73 times as large as for a direct-fired chiller.

Chapter 8: Conclusions

Summary of Accomplishments

The work described in this thesis resulted in a number of accomplishments. They are summarized below:

- The following ASPEN Plus models were produced. The two water/LiBr models are unique to ASPEN Plus. All three chiller models have acceptable discrepancies with EES values, with the two water/LiBr models having low discrepancies. The models produced are:
    - A single effect water/LiBr model which had less than a 3% discrepancy with EES models.
    - A double effect water/LiBr model which had less than a 5% discrepancy with EES models.
    - A single effect ammonia/water model which had less than a 7% discrepancy with EES models.
    - A turbine/chiller integrated model for each chiller design. The gas turbine model had less than a 5% discrepancy with experimental results.
- Three parametric studies were conducted. They give insight into how a gas turbine driven chiller operates under varied conditions. Results of these studies are provided graphically in Chapter 7. The studies conducted are:
    - A study on the effect of part loading on turbine efficiency and available waste heat

    - A study on the effect of varying evaporator temperature on chiller performance
    - A study on the effect of varying ambient conditions on chiller performance
- A study analyzing the performance of various chiller designs when driven by a gas turbine was conducted. From this study, it was concluded that the double effect water/LiBr cycle was best for this application.
- A seasonal study was performed which was able to determine the available cooling if a chiller used the available waste heat from the selected gas turbine. This study predicted that a double effect water/LiBr chiller could produce 435 GWh annually when driven by a GE MS5001 turbine. This translates to 43% of the cooling provided by the propane cycle, or 27% of the total cooling required in an APCI plant.

Conclusions

The research presented in this thesis investigates the potential to use gas turbine exhaust in LNG plants to drive absorption chillers. This thesis details the modeling process used to create three absorption cycle models in ASPEN: a single effect water/LiBr, a double effect water/LiBr, and a single effect ammonia/water model. These models were verified against EES models, showing small discrepancies (less than 5% for the water/LiBr models, less than 7% for the ammonia/water model). The two water/LiBr models are unique in ASPEN plus and

will give many advantages over models created in EES. They will be much more user-friendly and visually appealing to a casual user. They can be created quicker, and can be more readily integrated into larger processes. Finally, any assumptions made in model creation can be altered with modest effort as desired by the user.

Next, a waste heat source was selected to conduct analysis with. The GE MS5001 gas turbine was chosen because this turbine is commonly found in LNG plants. It is also the most attractive of waste heat sources in LNG plants, since gas turbine exhaust is plentiful and high temperature. The chiller models were connected to an existing gas turbine model to conduct analysis.

Various results were obtained from these models. First, parametric studies were conducted to ascertain the effect of part loading, evaporator temperature, and ambient conditions on chiller performance. Next, an analysis was done to evaluate which chiller design was the most utile. This analysis concluded that for this application, a double effect water/LiBr chiller is the best design to use. Finally, a seasonal study using Abu Dhabi weather data was conducted, predicting the performance of the MS5001 driven double effect water/LiBr chiller throughout the year. The total available cooling predicted is over 400 GWh annually. Because the savings are potentially so enormous, adding an absorption chiller to recover waste heat is a no-brainer.

Future Work

There are a number of potential extensions to this project that could give further insight. These extensions will be broken into two categories: improvements

that could be made to the models, either to improve accuracy or robustness, and further analysis that could be done with the models.

Model Improvements

- The first improvement that could be made would be to create double effect ammonia/water model. This would complete the library of available models. Such a model was not created because the imperfect property method used to model ammonia/water led to convergence issues with the single effect ammonia/water model. These effects would have been magnified with a double effect model.
- Other configurations could also be modeled; for example, a half effect or triple effect cycle.

Further Analysis with Models

- Other waste heat sources could be considered. These could include other sources identified within the LNG plant, or the models could be used for other projects. Since the temperature, quantity, and availability of the waste heat dictates the utility of using chillers to recover waste heat, studies with different waste heat source would result in different conclusions.
- The models could be directly integrated into and LNG plant cycle for completeness and further insight into the feasibility of such an improvement. This work is currently in progress at CEEE.

- A number of other uses for the cooling provided by the chillers could be considered. This work is also in progress at CEEE.

Bibliography

1. Brant, B., New waste-heat refrigeration unit cuts flaring, reduces pollution, Oil and Gas Journal, 1998, V. 96, N. 20, pp. 61-65.

2. Di Napoli, R. N., Gas Turbine Prove Effective as Drivers for LNG Plants, Oil and Gas Journal, 1980, V. 78, N. 31, pp. 47-52.

3. Edera, M., Development of a new gas absorption chiller heater-advanced utilization of waste heat from gas-driven co-generation systems for air-conditioning, Energy Conversion and Management, 2002, V. 43 , pp.1493–1501.

4. Hwang, Y., Potential Energy Benefits of Integrated Refrigeration System with Microturbine and Absorption Chiller, International Journal of Refrigeration, 2004, V. 27, N. 8, pp. 816-829.

5. Kowalski, G., Improving turbine performance by cooling inlet air using a waste heat powered ejector refrigerator, Proceedings of the ASME Advanced Energy Systems Division, 1996, V. 36, pp. 501-508.

6. Shih, H. Utilization of waste heat in the desalination process, Desalination, 2007, pp. 464-470.

7. Zogg, R., Using CHP systems in commercial buildings, ASHRAE Journal, 2005, V. 47, N. 9, pp. 33-36.

8. Spilsbury, C., Liu, Y, Petrowski, J. and Kennington, W., Evolution of Liquefaction Technology for today's LNG business, 7° Journess Scientifiques et Techniques, November 2006, Oran, Algeria

9. Vink, K., Nagelvoort, R., "Comparison of Baseload Liquefaction Processes", Twelfth Internation Conference and Exhibition on Liquefied Natural Gas, May 1998, Perth, Australia.

10. Domanski, P., "Theoretical Evaluation of the Vapor Compression Cycle With a Liquid-Line/Suction-Line Heat Exchanger, Economizer, and Ejector," U.S. Department of Commerce Report, 1995.

11. Srikhirin, P., Aphornratana, S., Chungpaibulpatana, S., "A review of absorption refrigeration technologies," Renewable and Sustainable Energy Reviews, Vol. 5, Issue 4, pp. 343-372.

12. Florides, G., Kalogirou, S., Tassou, S., Wrobel, L., "Modelling [sic] and Simulation of an Absorption Solar Cooling System for Cyprus," Solar Energy, Vol. 72, Issue1, pp. 43-51.

13. Hufford, P., “Absorption Chillers Improve Cogeneration Energy Efficiency”, ASHRAE Journal, Vol. 34, Issue 3, pp. 46-53.

14. Maidment, G., Tozer, R., “Combine Cooling Heating and Power in Supermarkets,” Applied Thermal Engineering, Vol. 22, Issue 6, pp. 653-665.

15. Moné, C., Chau, D., Phelan, P., “Economic Feasibility of Combined Heat and Power and Absorption Refrigeration with Commercially Available Gas Turbines,” Energy Conservation and Management, Vol. 42, Issue 13, pp. 1559-1573.

16. Sumathy, K., Huang, Z., Li, Z., “Solar Absorption Cooling with Low Grade Heat Source — a Strategy of Development in South China,” Solar Energy, Vol. 72, Issue 2, pp. 155-165.

17. Lazzarin, R.M., Gasparella, A., Longo, G.A., 1996, “Ammonia-Water Absorption Machines for Refrigeration: Theoretical and Real Performances”, International Journal of Refrigeration, Vol. 19, No. 4, pp. 239-246.

18. ABSIM, Oak Ridge National Laboratory, P.O. Box 2008, Oak Ridge, TN, USA.

19. Grossman, G., Zaltash, A., 2001, “ABSIM -- Modular Simulation of Absorption Systems,” International Journal of Refrigeration, Vol. 24, No. 6, pp. 531-543.

20. Beitelmal, M., Chandrakant, P., 2006, “Model-Based Approach for Optimizing a Data Center Centralized Cooling System,” HP Laboratories, Palo Alto, CA, USA.

21. Engineering Equation Solver, Version 8.176, F-Chart Software, Box 44042, Madison, WI, USA.

22. Yin, H., 2006, “An Absorption Chiller in a Micro BCHP Application: Model based Design and Performance Analysis,” Ph.D. Thesis, Carnegie Mellon University, Pittsburgh, PA, USA.

23. Liao, X., 2004, “The Integration of Air-Cooled Absorption Chiller in CHP Systems,” Ph.D. Thesis, University of Maryland, College Park, MD, USA.

24. Aspen Plus, Version 2006, Aspen Technology Inc., 200 Wheeler Road Burlington, MA, USA.

25. Darwish, N., Al-Hashimi, S., Al-Mansoori, A., “Performance Analysis and Evaluation of a Commercial Absorption-Refrigeration Water-Ammonia (ARWA) System”, International Journal of Refrigeration, Vol. 31, No. 7, pp. 1214-1223.

26. Reid, R., Prausnitz, J., Poling, B., “The Properties of Gases & Liquids,” 4th Edition, McGraw-Hill, 1988.

27. Haar, L., Gallagher, J., Kell, G., 1984, "NBS/NRC Steam Tables," CRC Press, Boca Raton.

28. *ASHRAE Handbook- Fundamentals*, Atlanta: American Society of Heating, Refrigerating and Air-Conditioning Engineers, Inc. 1989.

29. Glasstone, S., 1972. "Thermodynamics for Chemists," Krieger Publishing Co.

30. Kalinowski, P., 2007, "Application Analysis for a Waste-Heat Powered Absorption Refrigeration System in the LNG Recovery Process," Master's Thesis, University of Maryland, College Park, MD, USA.

31. Herold, K.E., Radermacher, R., and Klein, S, 1996, "Absorption chillers and heat pumps," CRC Press, Boca Raton.

32. Peng, D., Robinson, D., "A New Two-Constant Equation of State", Industrial & Engineering Chemistry Fundamentals, 1976.

33. Mortazavi, A., Rodgers, P., Hwang, Y., Radermacher, R., "Enhancement of LNG Propane Cycle through Waste Heat Powered Absorption Cooling", Pending Publication.

34. GE Energy, Gas Turbine Performances Data, 2007.

35. EnergyPlus, US Department of Energy, 1000 Independence Ave., SW Washington, DC, USA.

36. Mortazavi, A., Somers, C., Hwang, Y., Radermacher, R., Al-Hashimi, S., Rodgers, P., "Efficiency Enhancements of APCI base cycle by Absorption Chillers", Pending Publication.